NAVAL POSTGRADUATE SCHOOL
Monterey, California

THESIS

DEVELOPMENT AND CONTROL OF ROBOTIC ARMS FOR THE NAVAL POSTGRADUATE SCHOOL PLANAR AUTONOMOUS DOCKING SIMULATOR (NPADS)

by

Gary L. Cave

December 2002

Thesis Advisor: Michael G. Spencer
Second Reader: Brij N. Agrawal

Approved for public release; distribution is unlimited

THIS PAGE INTENTIONALLY LEFT BLANK

REPORT DOCUMENTATION PAGE			Form Approved OMB No. 0704-0188
Public reporting burden for this collection of information is estimated to average 1 hour per response, including the time for reviewing instruction, searching existing data sources, gathering and maintaining the data needed, and completing and reviewing the collection of information. Send comments regarding this burden estimate or any other aspect of this collection of information, including suggestions for reducing this burden, to Washington headquarters Services, Directorate for Information Operations and Reports, 1215 Jefferson Davis Highway, Suite 1204, Arlington, VA 22202-4302, and to the Office of Management and Budget, Paperwork Reduction Project (0704-0188) Washington DC 20503.			
1. AGENCY USE ONLY *(Leave blank)*	**2. REPORT DATE** December 2002	**3. REPORT TYPE AND DATES COVERED** Master's Thesis	
4. TITLE AND SUBTITLE: Title (Mix case letters) Development and Control of Robotic Arms for the Naval Postgraduate School Planar Autonomous Docking Simulator (NPADS)			**5. FUNDING NUMBERS**
6. AUTHOR(S) Gary L. Cave, LT, USN			
7. PERFORMING ORGANIZATION NAME(S) AND ADDRESS(ES) Naval Postgraduate School Monterey, CA 93943-5000			**8. PERFORMING ORGANIZATION REPORT NUMBER**
9. SPONSORING /MONITORING AGENCY NAME(S) AND ADDRESS(ES) N/A			**10. SPONSORING/MONITORING AGENCY REPORT NUMBER**
11. SUPPLEMENTARY NOTES The views expressed in this thesis are those of the author and do not reflect the official policy or position of the Department of Defense or the U.S. Government.			
12a. DISTRIBUTION / AVAILABILITY STATEMENT Approved for public release; distribution is unlimited			**12b. DISTRIBUTION CODE** A

13. ABSTRACT ***(maximum 200 words)***

This thesis encompasses the development of two robotic arms for integration onto the Naval Postgraduate School (NPS) Planar Autonomous Docking Simulator (NPADS) servicing vehicle. This research effort involved support structure design, fabrication, and construction, off-the-shelf motion control hardware integration, and control algorithm development and testing.

The NPADS system is being built as a test platform for spacecraft docking and capture mechanisms designed for autonomous rendezvous and servicing missions. As with the servicing vehicle, the robotic arms utilize a floatation system on an air-bearing granite table to provide a two-dimensional, drag-free environment. DC brushless servo motors serve as shoulder, elbow, and wrist joints allowing planar motion of the two-link arms. A National Instruments (NI) PXI computer and Motion Control card provide system processing and the software to hardware interface. The NI LabVIEW software suite enabled development of manual control code and autonomous control subroutines compatible with the control software of the NPADS main body. A single, wrist-mounted CCD bullet camera provides visual target acquisition for the robotic arm control system.

Testing and analysis were completed in the NPS Satellite Servicing Laboratory on a table-based test harness to facilitate initial design iteration.

14. SUBJECT TERMS Robotic Arms, Robotics, LabVIEW, Autonomous Docking, Satellite Servicing, Motion Control			**15. NUMBER OF PAGES** 111
			16. PRICE CODE
17. SECURITY CLASSIFICATION OF REPORT Unclassified	**18. SECURITY CLASSIFICATION OF THIS PAGE** Unclassified	**19. SECURITY CLASSIFICATION OF ABSTRACT** Unclassified	**20. LIMITATION OF ABSTRACT** UL

NSN 7540-01-280-5500 Standard Form 298 (Rev. 2-89)
Prescribed by ANSI Std. 239-18

THIS PAGE INTENTIONALLY LEFT BLANK

Approved for public release; distribution is unlimited

DEVELOPMENT AND CONTROL OF ROBOTIC ARMS FOR THE NAVAL POSTGRADUATE SCHOOL AUTONOMOUS DOCKING SIMULATOR (NPADS)

Gary L. Cave
Lieutenant, United States Navy
B.S., Georgia Institute of Technology, 1996

Submitted in partial fulfillment of the
requirements for the degree of

MASTER OF SCIENCE IN ASTRONAUTICAL ENGINEERING

from the

NAVAL POSTGRADUATE SCHOOL
December 2002

Author: Gary L. Cave

Approved by: Michael G. Spencer
Thesis Advisor

Brij N. Agrawal
Second Reader

Max F. Platzer
Chairman, Department of Aeronautics and Astronautics

THIS PAGE INTENTIONALLY LEFT BLANK

ABSTRACT

This thesis encompasses the development of two robotic arms for integration onto the Naval Postgraduate School (NPS) Planar Autonomous Docking Simulator (NPADS) servicing vehicle. This research effort involved support structure design, fabrication, and construction, off-the-shelf motion control hardware integration, and control algorithm development and testing.

The NPADS system is being built as a test platform for spacecraft docking and capture mechanisms designed for autonomous rendezvous and servicing missions. As with the servicing vehicle, the robotic arms utilize a floatation system on an air-bearing granite table to provide a two-dimensional, drag-free environment. DC brushless servo motors serve as shoulder, elbow, and wrist joints allowing planar motion of the two-link arms. A National Instruments (NI) PXI computer and Motion Control card provide system processing and the software to hardware interface. The NI LabVIEW software suite enabled development of manual control code and autonomous control subroutines compatible with the control software of the NPADS main body. A single, wrist-mounted CCD bullet camera provides visual target acquisition for the robotic arm control system.

Testing and analysis were completed in the NPS Satellite Servicing Laboratory on a table-based test harness to facilitate initial design iteration.

THIS PAGE INTENTIONALLY LEFT BLANK

TABLE OF CONTENTS

LIST OF FIGURES

LIST OF TABLES

THIS PAGE INTENTIONALLY LEFT BLANK

ACKNOWLEDGMENTS

The author would like to thank the following people for their invaluable support in the completion of this thesis:

Dr. Michael Spencer – For rescuing me from a life of simulation,

Dr. Brij Agrawal – For his outstanding sponsorship,

Air Force Research Lab (AFRL) – For their trust and assistance,

LCDR Bob Porter – For his friendship and countless sanity checks,

Mr. Glenn Harrell – For fabrication of the structural components of the arms,

and

Walter Cave – For re-teaching his stubborn son the electronics basics that he refused to learn growing up.

But, most importantly, I want to thank my wife and girls, Jessica, Kayla, and Corinne, for turning each day into a Beautiful, Sunny Day. Their unending love and support allowed me to complete this step in my life, making it all the more special.

THIS PAGE INTENTIONALLY LEFT BLANK

I. INTRODUCTION

The current design philosophy for most satellites involves developing a spacecraft that can support a given payload for a set number of years, usually between seven and ten, with the expectation that a follow-on spacecraft will be developed as the replacement by End of Life (EOL). The primary driver behind this philosophy is the perceived need for human involvement in repair and refueling operations. Since manned missions are restricted to shuttle-capable altitudes and inclinations, satellites that operate in the Medium Earth Orbit (MEO), Geosynchronous Earth Orbit (GEO), High Earth Orbit (HEO), and even Low Altitude Polar Orbit are not considered accessible for repair and replenishment.

The research involved in this thesis calls for a paradigm shift in satellite design. The Naval Postgraduate School and several other renowned research universities are exploring the feasibility of autonomous on-orbit docking of spacecraft and the use of robotic technology to enable repair and replenishment of vital systems and consumables, such as fuel. The Department of Defense and commercial ventures, alike, should be interested in the ability to readily extend mission life of the multi-million (or billion) dollar investments that they place in space. Improving productivity and cutting life cycle costs are the two primary goals of the new design philosophy. The following sections illustrate only a portion of the current research projects and operational equipment being developed toward these goals.

A. BACKGROUND

1. On-Orbit Spacecraft Docking

Spacecraft docking began in 1966 during the Gemini program and has continued throughout the life of the manned space program, including the current Shuttle-to-International Space Station (ISS) missions. Yet, every American docking mission to date has required human intervention, or "man-in-the-loop." However, in November 1997, the National Space Development Agency of Japan (NASDA) launched Engineering Test Satellite VII (ETS-VII), a set of two satellites, the chaser and target, placed in a 550

kilometer, circular orbit to test the feasibility of autonomous spacecraft docking [Ref. 1]. The two satellites (shown in Figure 1) were launched together, separated on orbit, and the chaser maneuvered to recapture the target. Though some of the experimentation involved earth-based telerobotic commands vice pure autonomous control, ETS-VII provided an on-orbit demonstration of the capabilities required for future ventures.

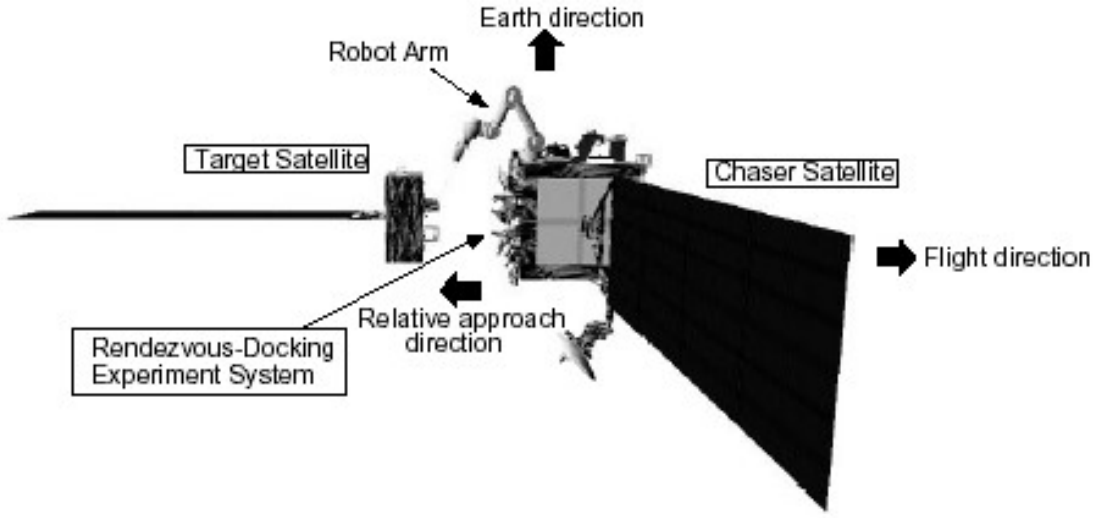

Figure 1 Engineering Test Satellite VII (After: Ref. 1)

A variety of organizations, including the National Aeronautics and Space Administration (NASA) and the Defense Advanced Research Projects Agency (DARPA), have projects ongoing in the area of autonomous docking. NASA's Space Launch Initiative to develop safer more affordable methods of space travel spawned the Demonstration of Autonomous Rendezvous Technology (DART) program from Orbital Sciences Corporation. This project will test a completely autonomous control routine to raise a chase vehicle to an orbit near its target, move the vehicle within fifteen meters of the target to test station-keeping abilities, and then demonstrate collision avoidance maneuvering. Meanwhile, DARPA's Orbital Express mission initiated development of the ASTRO vehicle, a prototype servicing satellite, as well as projects at a number of universities, including the University of Maryland's RANGER program, also investigating the use of robotics for spacecraft servicing.

Beyond the high profile projects listed above, Stanford University has developed the Multi-Manipulator Free Flying Space Robots to test cooperative control of multiple vehicles in capture and servicing operations. The University of Washington Department of Aeronautics and Astronautics utilized a class design project to develop a shuttle-based demonstration of on-orbit autonomous control, the On-Orbit Autonomous Satellite Servicer (OASiS). And the Naval Postgraduate School Department of Astronautics hosts a joint facility with the Air Force Research Laboratory to develop the NPS Planar Autonomous Docking Simulator (NPADS) system described later in this chapter.

2. Space-Based Robotics

As with on-orbit docking, robotics has a reasonable legacy in space, beginning in earnest in the early 1980's with the addition of the Shuttle Remote Manipulator System (SRMS). Further developments have included CanadaArm, or the Space Station Remote Manipulator System (SSRMS), and the Japanese Experiment Module Remote Manipulator System (JEMRMS) both built for the International Space Station. These three systems, however, involve large mass, large volume components and require the involvement of a human operator. Even the Special Purpose Dexterous Manipulator (SPDM) illustrated in Figure 2, being developed by Canada to accomplish delicate maintenance and servicing tasks aboard ISS, requires a member of the ISS crew to conduct operations.

Figure 2 Special Purpose Dexterous Manipulator (From: Ref. 2)

Further, smaller robots being developed by NASA (Robonaut, illustrated in Figure 3) and the University of Wisconsin (GOFER) to assist astronauts during extravehicular activity (EVA) still require a human operator. The design driver is to reduce the number of EVAs required of the shuttle or ISS crew, by replacing one of the two astronauts currently required for each EVA with a robot assistant, in order to minimize space exposure and increase the level of safety. Robonaut is a highly advanced robotic assistant that provides more than forty-five degrees of freedom, over 150 sensors, and two fully dexterous hands; but, the fact remains that two astronauts are required still for each EVA, the second being on-station (or in the shuttle) utilizing virtual reality interfaces [Ref.3].

Figure 3 Robonaut (From: Ref. 3)

In order to minimize the risks (i.e., human error) and risk factors (i.e., fatigue) created by human involvement, autonomous operations by highly precise robotic systems are required. Terrestrial organizations have moved to robotic systems for repeatable tasks requiring high precision in manufacturing, industrial inspection, and even surgical applications. Space-based robotics must follow this course. Again, the ETS-VII mission included experimentation with earth-based operators commanding the robotic arm attached to the chaser vehicle, but there is a significant time delay between command and output, further proving the need for a fully autonomous system. This thesis provides the

initial design of a robotic arm motion control assembly for integration into the NPADS system, with the vision of future development into a completely autonomous control scheme.

3. Naval Postgraduate School (NPS) Satellite Servicing Laboratory

The Satellite Servicing Laboratory (SSL) is the newest of four laboratories included within the Spacecraft Research and Design Center (SRDC) at the Naval Postgraduate School. The mission of the SSL is to investigate technologies developed toward on-orbit rendezvous of spacecraft with the goal of prolonging spacecraft operational life. The Satellite Servicing Laboratory served as host for the research conducted for this thesis. The Naval Postgraduate School (NPS) Planar Autonomous Docking Simulator (NPADS) system provides the focus of research in the SSL and is jointly funded by NPS and the Air Force Research Laboratory (AFRL).

B. NPS PLANAR AUTONOMOUS DOCKING SIMULATOR (NPADS)

The NPADS program was started in order to provide an autonomous servicing spacecraft test platform. It is envisioned that the NPADS system will serve as a functional 2D simulator for validation of advanced control algorithms, docking mechanisms, manipulators, and any other software or hardware developed for space rendezvous, docking, and repair missions. As part of initial development of this lab, research was divided into two areas: control of the main servicing vehicle and control of the capture and manipulation devices (robotic arms). Figure 4 provides an illustration of the NPADS design concept; as shown in the figure, the NPADS system will eventually expand to include a target vehicle as well.

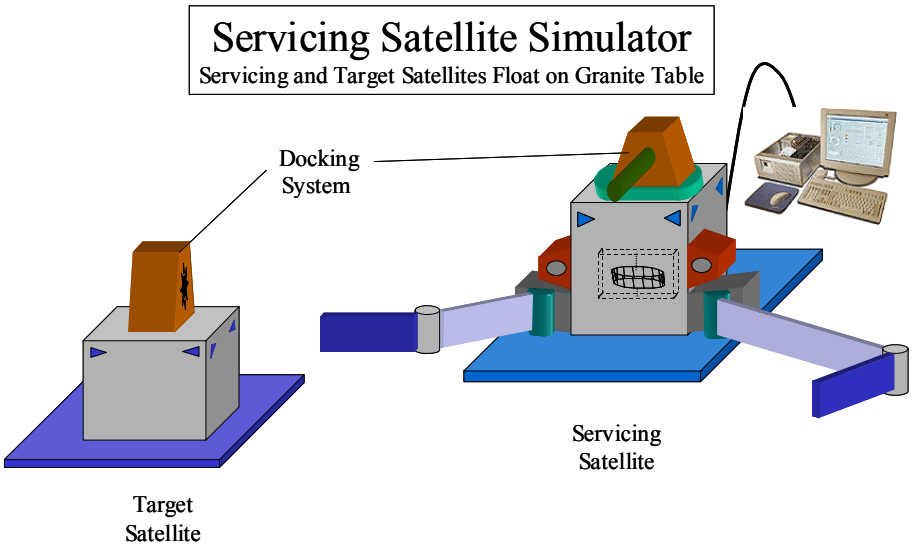

Figure 4 NPADS Design Concept

1. Servicing Vehicle

The first thesis produced from the NPADS system provided the design of the servicing vehicle main body and an initial PD control law designed for autonomous operation of the vehicle [Ref. 4]. The NPADS main body concept is depicted in Figure 5.

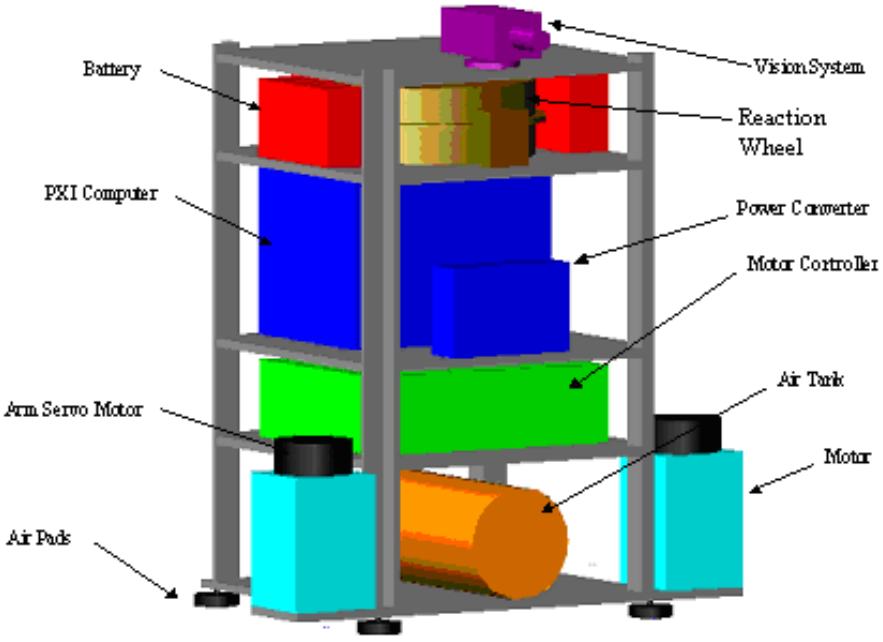

Figure 5 NPADS Servicing Vehicle Concept

a. Hardware

The NPADS servicing vehicle utilizes a compressed air system to provide floatation of the vehicle on an air-bearing granite table, thus providing two dimensional freedom of motion, simulating a 2D space environment. The vehicle includes an onboard PXI computer for control, which makes use of a reaction wheel and eight gas thrusters to regulate position and orientation. A black and white CCD camera, acting as a star sensor, and a MEMS angular rate sensor provide feedback to the attitude determination and control program. To provide freedom of motion and total autonomy, all of the systems operate on DC power provided by two lead-acid batteries and a series of voltage converters. A wireless Ethernet connection allows the control computer to offload data for processing by an off-board workstation. The vehicle also includes a forward-looking CCD camera for target detection, though this device has not yet been implemented.

b. Software

The NPADS main body has both manual control and autonomous control programs. These algorithms were developed using the National Instruments LabVIEW software suite.

2. Robotic Arms

This thesis provides the characteristics for the two robotic arms designed for integration onto the servicing vehicle. The initial design concept is illustrated in Figure 6.

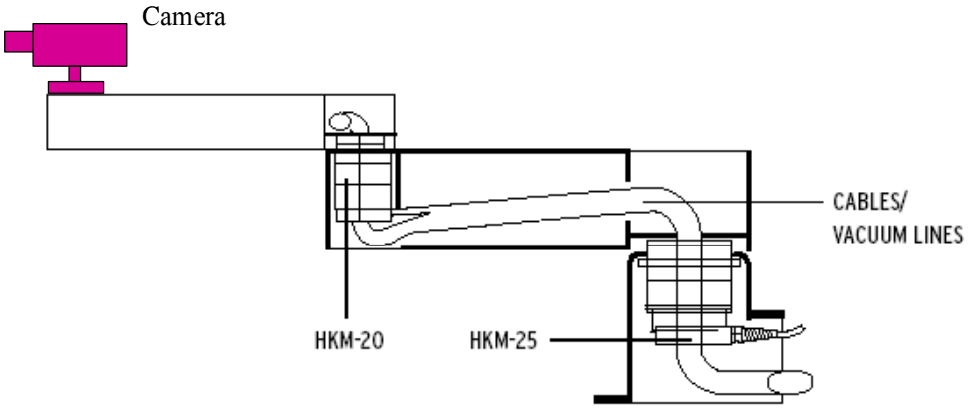

Figure 6 NPADS Robotic Arm Design Concept (After: Ref. 5)

a. Hardware

The NPADS robotic arms consist of a two-link, three-joint architecture offering three degrees of freedom. Utilizing pre-existing technology for the system components, the arms use three DC hollow-shaft brushless servo motors, which act as the shoulder, elbow, and wrist joints, with worm gearing and integrated optical encoders for position and velocity feedback to the control code. Three servo amplifiers translate the control voltages into a three phase distribution to move the joint motors. The arms float on the air-bearing table using an identical compressed air system as the main body, allowing for immediate integration of the arms. A PXI control computer and PXI-technology motion control card are used to control the arms. And, again, all components utilize DC power such that the system is autonomous. A black and white CCD camera is mounted to the left wrist joint motor shaft for target acquisition. Currently, there are no manipulation or capture devices implemented on this system.

b. Software

As with the control code of the main body, the National Instruments LabVIEW suite, including the FlexMotion and IMAQ modules, was used for software development. Control code programming included a manual control system and several autonomous control algorithms for eventual integration with the main body control code.

C. SCOPE OF THESIS

This thesis comprises the work involved in the design, construction, and initial control software programming of two robotic arms for the NPADS servicing vehicle. This effort is one of the first phases of development of a fully autonomous, neural network-based, rendezvous and docking test platform. This is the second thesis written in relation to the NPADS system.

Following initial research regarding motion control systems, two robotic arms were constructed using various off-the-shelf motion control components. This step involved design and fabrication of a structural support frame and test yoke, creation of a variety of wiring harnesses to integrate the components, and stage-by-stage testing of component interfaces. Upon completion of hardware integration, the first arm was wired

to the control computer in order to accomplish electronic tuning of the joint motors and initial testing of the system using pre-programmed software. Once system integrity was established, a manual control code was built and tested; then, several autonomous control subroutines designed for integration into the NPADS control architecture were developed. Finally, a vision system was integrated to provide target acquisition. This research concluded with successful testing of each of the control algorithms and integration of the first arm onto the NPADS servicing vehicle. The second arm was connected to the test harness for future development and research.

THIS PAGE INTENTIONALLY LEFT BLANK

II. HARDWARE & INTEGRATION

The robotic arms for the NPADS servicing vehicle were designed to operate either while the arms were attached to the NPADS vehicle (Figure 7) or while attached to a test structure (Figure 8) for independent testing of the arms. Modularity, interoperability, size, and cost were drivers for the components selected. This chapter describes the individual hardware components used in the design of the NPADS robotic arms and their integration into the system.

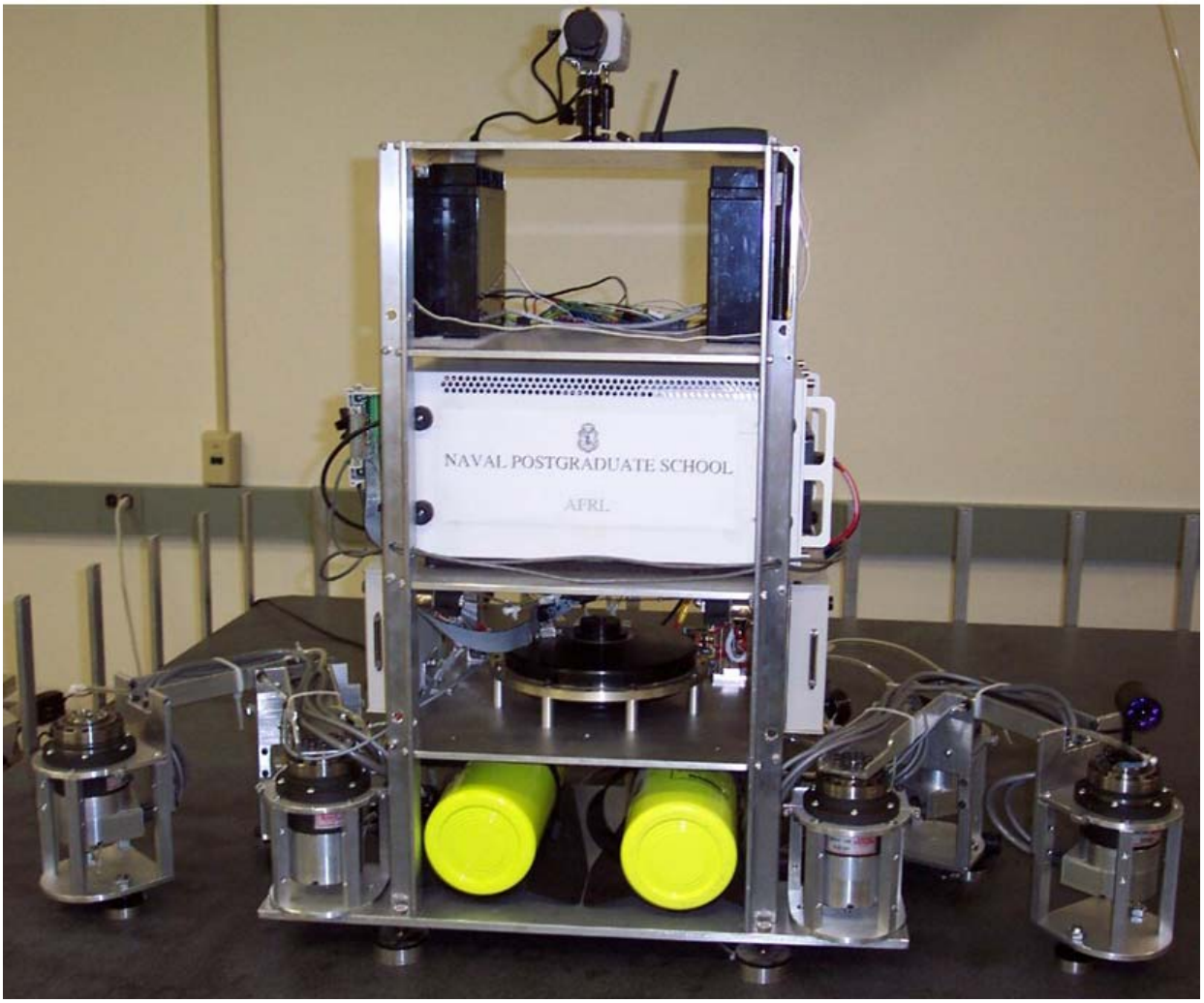

Figure 7 NPADS Vehicle with Robotic Arms

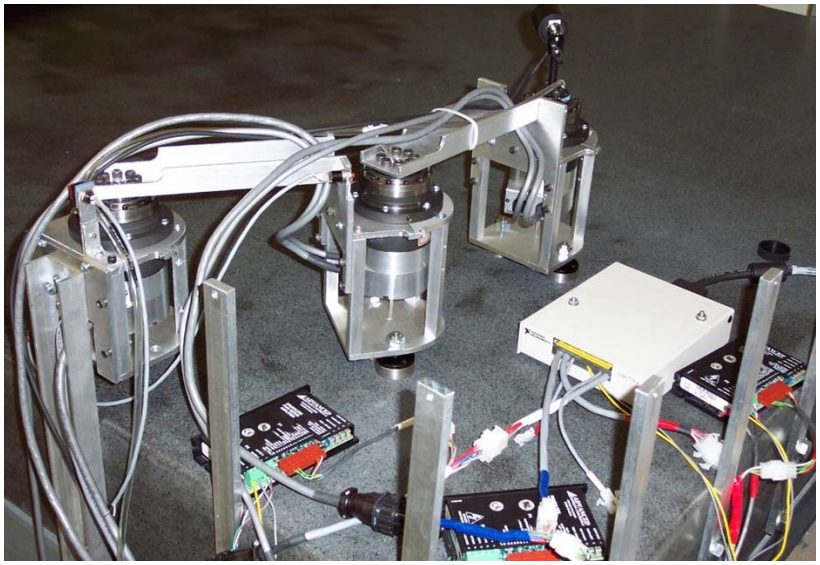

Figure 8 Robotic Arm Attached to Test Harness

A. OVERVIEW

As with the NPADS vehicle, commercial-off-the-shelf (COTS) components were used to alleviate the need for major modification, drive down cost, and minimize the risk of interoperability problems. Since this project was aimed at creating a test-bed for further research of docking systems and manipulation devices, time was a critical factor that led to the use of COTS items to develop the simulator as efficiently as possible. Similarly, the simulator was initially designed for use in a confined space (a 6' x 8' granite air-bearing table), thus defining a need to keep the components as small as feasible.

Again, the NPADS robotic arms were designed to mate to the base plate of the NPADS servicing vehicle as well as a test harness, as shown in the earlier figures. The 3-joint (shoulder, elbow, wrist), 2-link design is depicted in Figure 9. Each link consists of a motor support structure, a rigid interjoint link, 2 floatation air pads, a DC Brushless Servo motor, and a 3-phase amplifier. The inputs and outputs from the joint motors and their associated amplifiers are connected to a Universal Motion Interface which connects to a Motion Control Card in the Onboard Control Computer. The wrist of the left arm has a black and white wide field-of-view bullet camera attached which is connected to the Onboard Control Computer via an Image Acquisition Card. These components are

described in detail below. Table 1 contains a summary of the characteristics of the components.

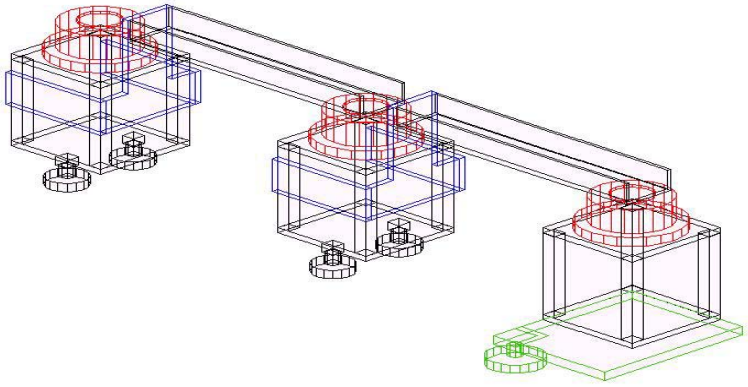

Figure 9 Conceptual Drawing of Robotic Arm Design

Table 1 NPADS Robotic Arm Component Characteristics

	Parameter	Value
Physical Attributes	Overall Length[1]	20.5 in
	Overall Width[2]	5.25 in
	Width Stowed[3]	15.5 in
	Height	9 in
	Mass[4]	22 lb
Motion Control	Motor Type	DC Brushless Servo
	Operating Voltage	24 V
	Operating Current[5]	0.2 A
	Rated Torque[6]	115/233 in-lb
	Gear Ratio[6]	50:1/100:1
	Feedback Method	Optical Encoder
	Amplifier[7]	PWM Servo Amplifier
	Operating Voltage	24 V
	Max Continuous Current	6 A
	Universal Motion Interface[8]	4 axis
	Operating Voltage	5 V
	Operating Current	0.5 A
Computer System	Computer	National Instruments PXI
	Processor	866 MHz Pentium III
	Data Acquisition Cards	Motion Control/Vision
	Voltage	24 V (DC or AC)
Vision System	Target Alignment Camera	ProVideo Bullet CCD
	Shutter Speed	100 Hz

1. From center of shoulder joint to center of wrist joint
2. At joint
3. Measured from side of NPADS vehicle
4. Does not include mass of amplifiers
5. Current is dependent on required torque
6. Shoulders are higher torque/higher geared motors than elbow and wrist motors
7. One amplifier per joint (six total)
8. One UMI per arm (2 total)

B. STRUCTURES

The joint motor support structure was constructed using 6061-T6 Aluminum and was designed to minimize weight and height, while providing the structural integrity necessary for the expected torques placed on the joints. Each support structure is comprised of a 1/4-inch base plate which supports 2 air pads (elbow and wrist only), a 1/4-inch split top plate with tensioning screws to mate around the joint motor housing, a 1/4-inch back plate (elbow and wrist only) that allows for connection to the link, and four 1/2-inch square rods acting as standoffs. Since the shoulder joint drives the height of the arm, the elbow and wrist standoffs were designed such that their air pads would be even with the granite table when the floatation system was off. The frame uses 10-32 screws to connect the individual pieces.

The arm links are again constructed of 6061-T6 Aluminum. The links are 2-inch by 1-inch by 1/8-inch channel, 9-inches long. In one end, holes are drilled for mounting to the joint motor shaft, in the other, mounting holes allow connection to the back plate of the next joint motor support with a groove cut such that the joint motor wiring harnesses can reside within the channel. The link to back plate connection is made using 10-32 screws, the link to motor connection is accomplished using M6 screws. Figure 10 illustrates the joint motor support structure and joint linkages. Appendix A contains detailed drawings of these structural components.

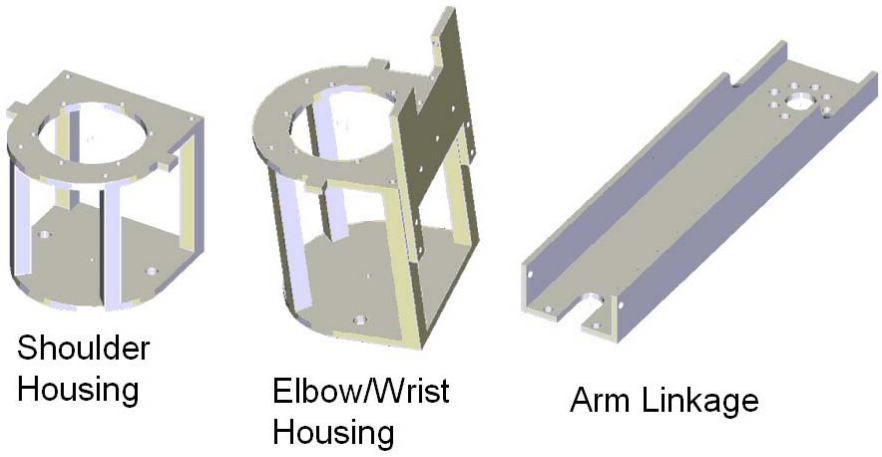

Figure 10 Structural Components

C. FLOATATION COMPONENTS

1. Air Pads

In order to simulate the space environment, the arms either had to support their own weight such that no contact was made with the granite table or a floatation system was needed to minimize the effects of drag. For simplicity and weight reduction, the second option was chosen. The vehicle and arms rest on an air-bearing granite table. The shoulder joint attaches directly to the vehicle frame and is supported by four 2-1/8 inch (55 mm) air pads that levitate the vehicle. The elbow and wrist support structures each connect to two 1-9/16 inch (40 mm) air pads. These air pads, manufactured by Aerodyne Belgium, provide a 20-micron cushion of air between the pads and the table that allow the joints to glide relatively friction-free across the table.

2. Air Supply System

Compressed air is supplied to the arm air pads at between 40 and 70 psi when attached to the vehicle due to a common supply line, and at 5 to 10 psi when attached to the test harness. This air is supplied via a 19 cu. ft. scuba tank, which supplies air at 3000 psi, a standard scuba first-stage regulator(ScubaPro Mk 16), which reduces pressure to 150 psi, and an in-line LP-LP regulator, made by Teco Pneumatic, which further reduces the air to usable ranges. The in-line regulator can be set to provide from 0 to 150 psi. The system weight determines the pressure needed to provide unobstructed motion.

The air is provided from the tanks to the air pads through a system of polyurethane tubing. Coming off the Mk 16 regulator is 1/4 ID x 3/8 OD tubing which connects to the in-line regulator. From the output of the second regulator, the tubing is reduced to 1/8 ID x 1/4 OD and, down again, to 1/16 ID x 1/8 OD which connects to the input of the air pads. Various polyurethane junctions (Ys and Ts) are used to connect the tubing. The material used for the links allows the tubing to reside inside the channel reducing the likelihood of snagging and wear. Figure 11 shows the air supply system and joint motor air pads.

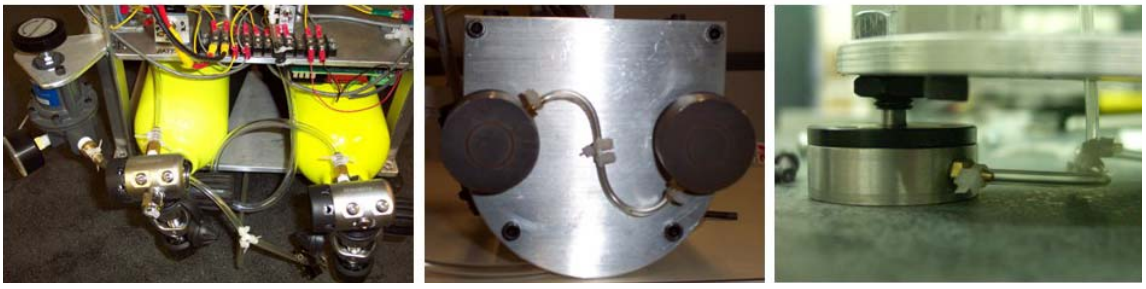

Figure 11 Floatation Components

D. POWER COMPONENTS

The overriding goal of this research was simulating autonomy. In keeping with this goal, all system components run on DC power, such that batteries could be used to provide the power necessary to run the entire vehicle and the arms. A system of two Panasonic 12-Volt, 20-Amp hour lead-acid batteries are wired in series on the vehicle to provide a 24-Volt output. The battery layout is provided in Figure 12.

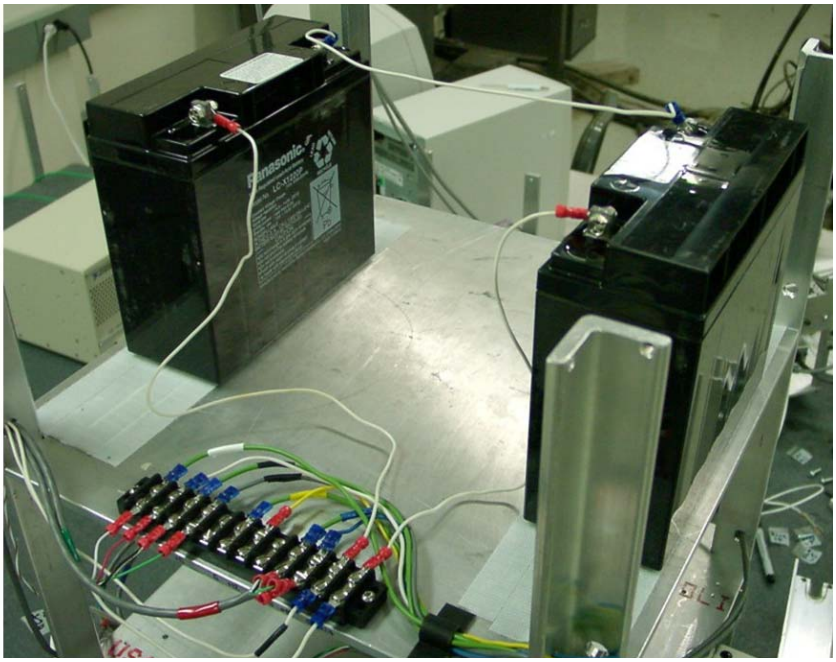

Figure 12 NPADS Batteries

A system of DC-DC converters is used on the vehicle to provide ±5V, +6V, +12V, and +18V required for various components of the NPADS vehicle. The joint motors, amplifiers, and control computer run directly off the batteries at 24V. However,

the Universal Motion Interfaces need 5V input and the bullet camera requires 12V. Due to the direct feed of 24V off the batteries, it was necessary to install a master switch that isolates power from the system; however, so that testing of the NPADS vehicle could be conducted without powering the arms, a second set of switches were installed such that the arms can be electrically isolated from the vehicle. A barrier strip is located on the rear of the second shelf of the vehicle to provide a centralized distribution point for the voltages required. Figure 13 illustrates the power distribution layout for the robotic arms. Table 2 delineates the layout of the barrier strip for arm power.

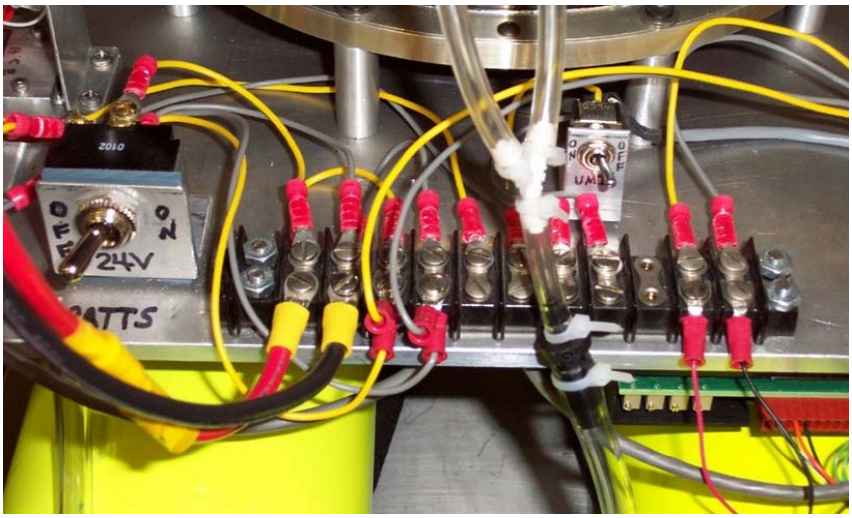

Figure 13 Power Isolation & Distribution Components

Table 2 Arm Power Distribution Barrier Strip Diagram

1	2	3	4	5	6	7	8	9	10	11
24V	GND	24V	GND	24V	GND	5V	GND	open	24V	GND
Master to Comp.	Master to Comp	Master to Arm Isol.	Master to Arm Isol.	Arm Isol to L Arm	Arm Isol to L Arm	DC-DC to UMI	DC-DC to UMI	N/A	Arm Isol to R Arm	Arm Isol to R Arm

E. MOTION CONTROL COMPONENTS

Motion Control consists of a command being developed in software, sent from an I/O board to a breakout box, interpreted by an amplifier, and further subdivided into commands (voltages) that can be understood by an electromechanical device (i.e., a joint motor). In the process of designing a motion control system, many options are available,

primarily in choosing the joint motor: multi-degree-of-freedom motors, stepper or servo motors, brushless or brushed motors, et cetera. The design goals for this research focused on a compact solution that would provide motion in one axis at a projected torque threshold and that the motion control system would have full compatibility with the control system of the NPADS vehicle. These criteria led to the selection of the components described in the following sections. Figure 14 illustrates the location of the various components on the NPADS vehicle. Appendix B provides wiring information for the motor harnesses, amplifier, and UMI.

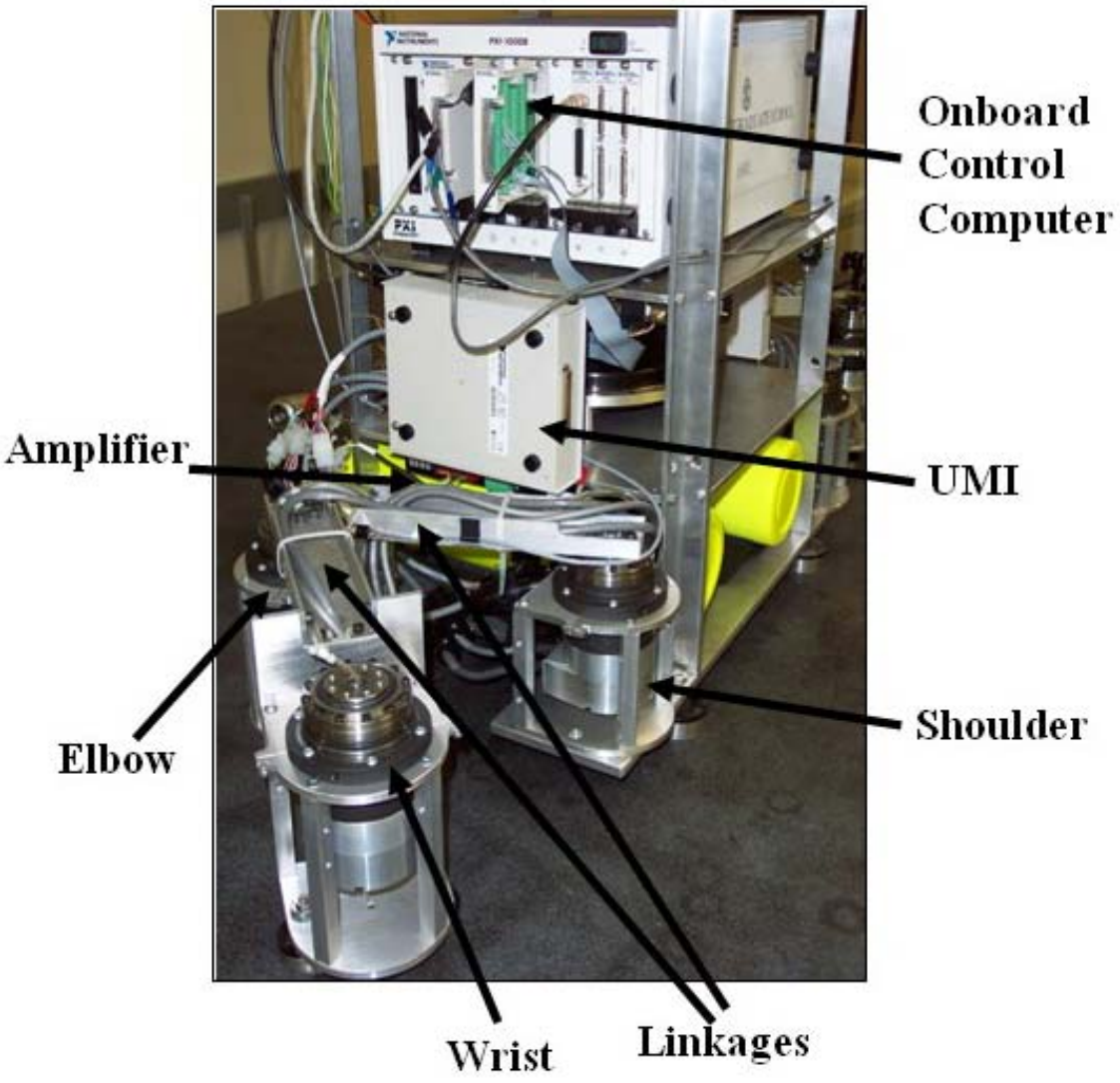

Figure 14 Motion Control System Layout

1. Joint Motors

Harmonic Drives PowerHub Hollow Shaft Brushless DC Servo motors (Figure 15) were selected for the joint motors. Two models, HKM-20-30 and HKM-20-60, are used for the shoulder joints and elbow/wrist joints, respectively. The HKM-20-30 model provides approximately twice the torque (233 in-lb or 26 N-m) of the other model; as with a human arm, the shoulder of a robotic arm needs to be the strongest joint in order to handle the loads caused by displacement. Externally, there is no distinction between the two motors.

Figure 15 Harmonic Drive DC Brushless Servo Motor

These motors were chosen for a variety of reasons. First, the joint motors needed to run on DC power in order to maintain autonomy. Second, a servo motor provides a smoother motion than a stepper motor since it possesses a limitless number of acceptable positions. Servo motors are penalized in accuracy and repeatability; but with the limited range of motion required for this test bed, these factors have little impact. Third, the hollow shaft design was key to running the air supply lines to the air pads at the elbow and wrist joints. Fourth, brushless motors work by means of electronic commutation. Since there is no physical contact, wear on the motor is reduced. Finally, these motors provide internal worm gearing, at a 100:1 ratio for the shoulders and a 50:1 ratio for the

elbows and wrists, and an integrated optical encoder (4000 counts/rev of drive shaft). The addition of these two subcomponents greatly simplified the prospect of component integration and interoperability.

2. Amplifiers

Advanced Motion Controls B15A Series (B12A6L) Brushless Servo Amplifiers are used to interface between the controller and the motors. Each joint motor requires a separate servo amplifier (Figure 16). The amplifier receives commands from the controller which are converted to a three-phase voltage output to the motor to control electronic commutation as desired, while receiving input from the motor's Hall sensor, which tracks the commutation of the motor, for feedback.

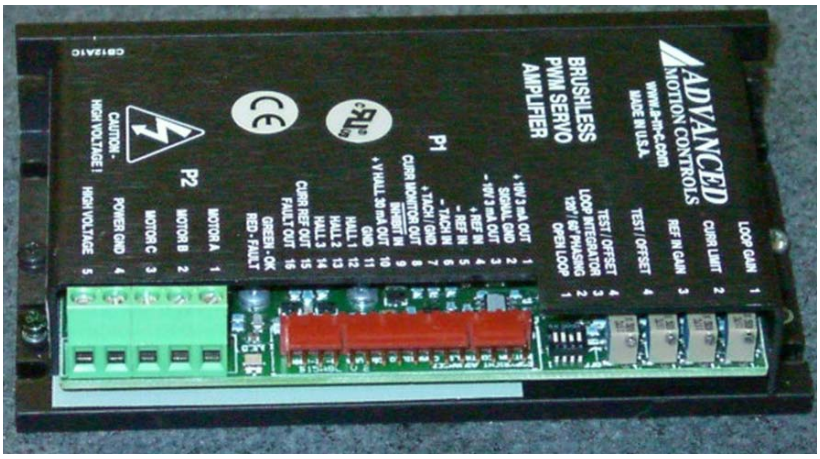

Figure 16 B12A6 Servo Amplifier

3. Universal Motion Interfaces

The Universal Motion Interface (UMI-7764) is a National Instruments connectivity accessory that connects the servo amplifiers, motors, encoders, and switches for up to four axes to the associated plug-in motion control board (PXI 7344) [Ref. 6]. Each arm requires a separate UMI. Figure 17 shows a UMI with one arm (3 axes) wired. The wiring layout of the UMI is included in Appendix B.

Figure 17 Universal Motion Interface

4. Home Switches

As mentioned previously, the optical encoder is located on the drive shaft of the joint motors. Consequently, there are multiple Index signals per single revolution of the output shaft, therefore it is impossible to identify a repeatable reference location at power-up using the encoders. To alleviate this problem, a series of Normally Off-Momentary On switches were placed at the parked (power-up) position of the shoulder and elbow joints so that software could be developed to find home, the repeatable reference position, each time the system were initialized. This function will be further defined in a later section. Figure 18 shows one of these switches.

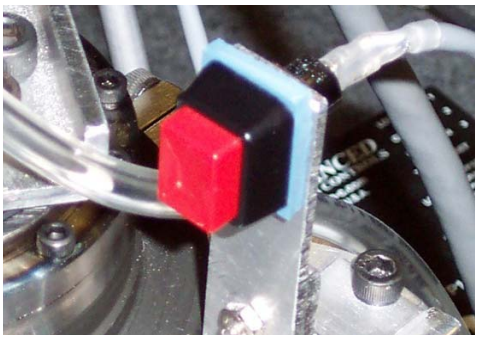

Figure 18 Home Switch

F. COMPUTER AND ASSOCIATED COMPONENTS

1. Chassis and Controller

On the second level of the NPADS vehicle, an onboard computer is mounted which controls all vehicle operations including motion control of the robotic arms. The computer, made by National Instruments, includes a chassis (1000B), controller (PXI (PCI eXtensions for Instrumentation) 8175), and various input/output cards described below. The 1000B chassis allows for both AC and DC operation and includes a controller interface and seven expansion slots for additional cards. The PXI 8175 controller is driven by an 866 MHz Pentium III processor, includes a hard drive, 3-1/2 inch floppy drive, Ethernet port, USB ports, and the standard interfaces of a desktop computer, and operates under the Windows 2000 operating system. PXI technology allows for a much more compact system by pushing many of the specialized functions to the expansion cards for processing. Figure 19 shows the onboard computer.

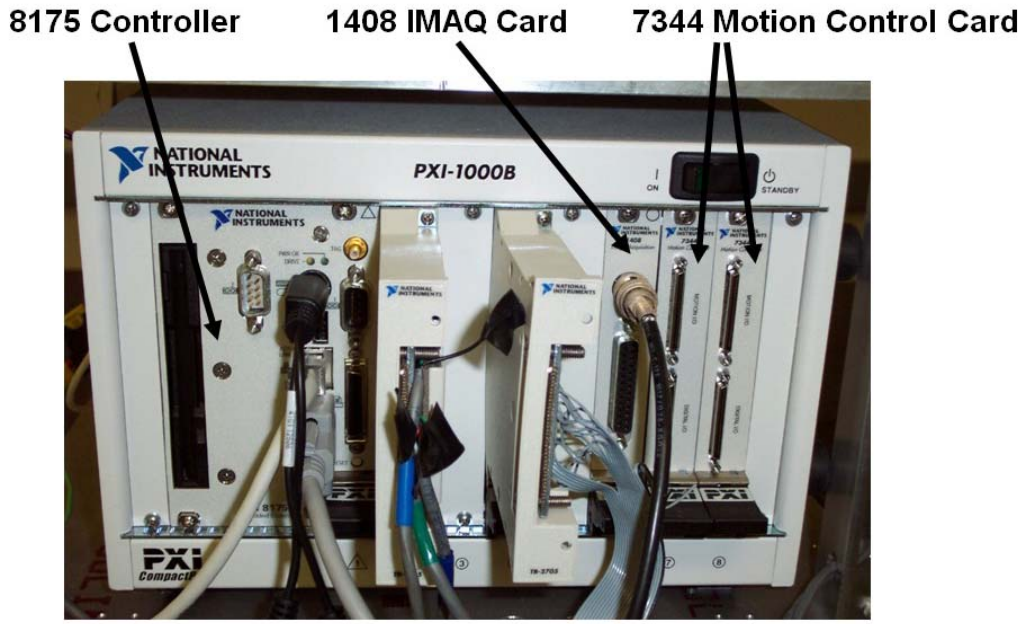

Figure 19 NPADS Onboard Computer

2. PXI 7344 Motion Controller Card

The PXI 7344 Motion Controller uses a dual-processor architecture with high speed communications to allow on-card processing of up to four axes (motors), either

stepper or servo, executing up to ten simultaneous motion programs, with 62 microsecond PID/PIF servo updates, encoder feedback up to 20 MHz, and various limit and trigger inputs [Ref. 7]. Each Motion Controller drives one robotic arm since there are three joint motors (axes) per arm. The 7344 board connects to a UMI via a 68-pin VHDCI connector.

3. PXI 1408 Image Acquisition (IMAQ) Card

The PXI 1408 is a monochrome IMAQ board that supports up to four video inputs from most standard video sources, using 8-bit flash analog to digital conversion to acquire and store an image [Ref 8]. The left robotic arm includes a black and white camera, mounted on the wrist, which provides video input to the PXI 1408 card. The 1408 board connects to the camera via a BNC connector.

4. Test Computer

For operation in the test harness, a second National Instruments computer is used. This computer consists of a 1002 chassis, an 8156B controller, one 7344 Motion Control Card, and a PXI 1408 Image Acquisition Card. The 1002 chassis is smaller, with only three expansion slots, and operates only on AC. The controller is driven by a 333 MHz MMX processor [Ref. 9] originally operating with the Windows NT operating system; however, an upgrade was conducted to Windows 2000 for interoperability. This computer is responsible solely for offboard testing of the robotic arms. The test computer is shown in Figure 20.

Figure 20 Robotic Arm Test Computer

G. VISION COMPONENTS

A ProVideo CVC-320WP CCD camera is attached to the wrist of the left robotic arm and is used for target acquisition/position verification. The camera contains a 1/3 inch fixed focal length image sensor that operates at a shutter speed of 100 Hz. The bullet camera is powered by 12 VDC. Figure 21 shows the camera mounted on the left wrist.

Figure 21 Robotic Arm Bullet Camera

III. CONTROL SOFTWARE

Development of software for the NPADS robotic arm motion control system was accomplished using the National Instruments LabVIEW 6i software suite and associated modules. By leveraging a single vendor for both hardware and software for much of the motion control system, interoperability and translation problems were bypassed. National Instruments PXI technology is based on:

> … an architecture that supports mechanical, electrical, and software features tailored to industrial instrumentation, data acquisition, and automation applications [Ref 9, 1-3].

Through backplane interfacing with the various specialty control boards, the PXI controller is able to schedule tasks more efficiently. LabVIEW was developed by National Instruments to take advantage of this architecture.

LabVIEW is a graphical programming language; unlike traditional languages such as FORTRAN or C, LabVIEW uses a series of icons, which are visual representations of commands or subroutines, and a wiring tool to connect icons to one another to create a functional program. For many of the specialty control boards, modules are included in the LabVIEW suite for function-specific commands; for example, the 7344 Motion Control card uses many commands included in the FlexMotion module – these commands are tailored for motion control applications. The chapter that follows discusses the development of the LabVIEW control program and subroutines designed for operation of the NPADS robotic arms.

A. OVERVIEW

The motion control program was developed in several stages. Initially, once hardware integration was completed, it was necessary to calculate the gains for each joint motor to ensure stable operation. Normally an intensive set of calculations using experimental data and basic control equations is required; however, LabVIEW includes a tool called the Measurement & Automation Explorer (MAX) which contains a set of sub-programs, as part of the FlexMotion software module, designed to test servo motors and

identify gains and other useful parameters. Thus, the relatively difficult task of tuning the joint motors was simplified greatly through the automated method included in the software suite. Next, to verify operational stability and test the ability to control the motors, a Manual Control program was developed using standard LabVIEW commands in conjunction with those in the FlexMotion module. Finally, a series of autonomous subroutines were developed for eventual use in the NPADS robotic arm onboard control program. Though manual control was tested briefly on the NPADS vehicle to verify telerobotic control, all tests and operations using the autonomous code to date have been conducted on the test harness.

B. MOTOR TUNING

Measurement & Automation Explorer is a versatile tool used to ensure proper, efficient interaction between computer hardware, software, and third party functional hardware. Figure 22 shows the MAX Configuration menu for the test computer. Under the Devices and Interfaces folder are subfolders for the computer ports and the two expansion cards: IMAQ PXI-1408 and PXI-7344. Also, under the 7344 subfolder, the various functional folders for Motion Controller setup and initialization can be seen. In short, the Device Resources folder provides motion controller to chassis interface information, Default 7344 Settings (see Appendix C) enables the user to input specifics of third party motors and feedback devices such that signals can be passed between the controller and these components (an example is presented in Figure 23), the Interactive folder provides the option of 1-D or 2-D manual control of joints for testing connectivity, and Calibration includes the tools for automatically or manually tuning servo motors.

Figure 22 Measurement & Automation Explorer Configuration Menu

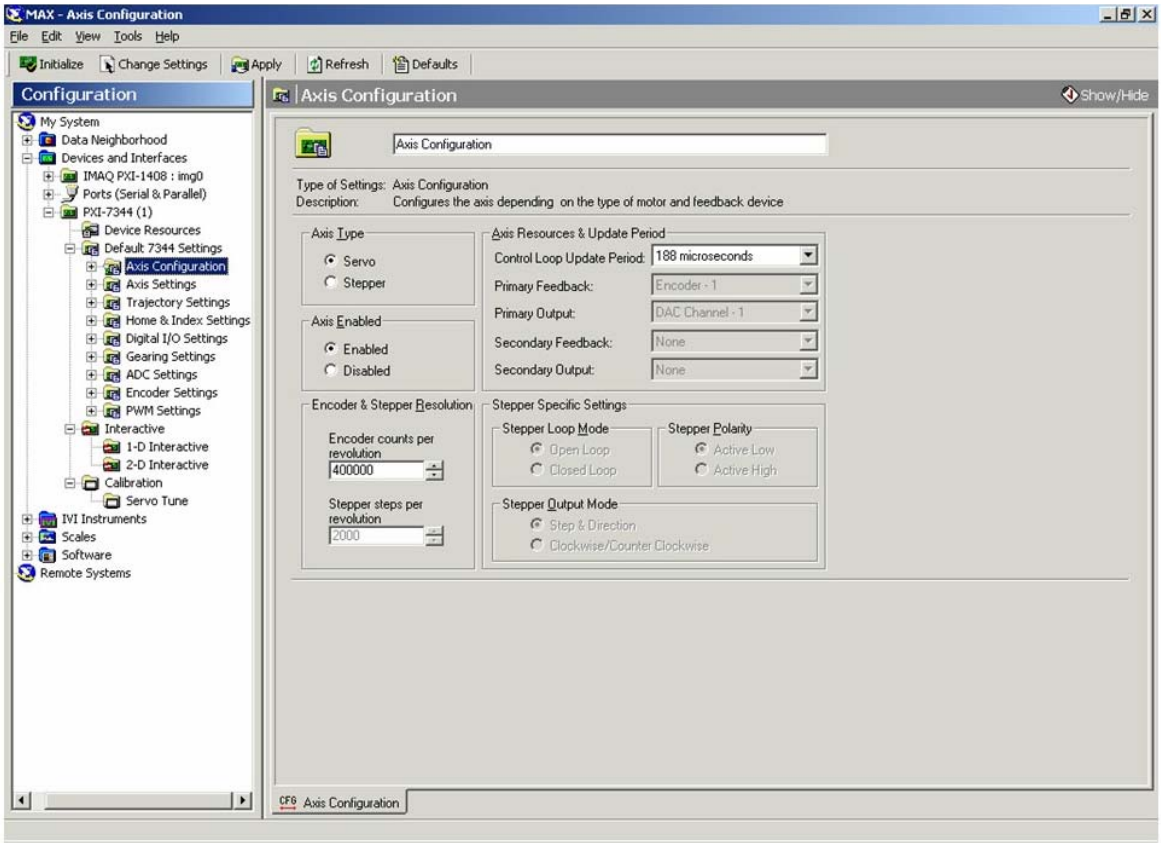

Figure 23 MAX Default 7344 Setting Axis Configuration Menu

The only option under the Calibration folder is Servo Tune, which contains five pages for various control settings and testing. The first of these pages is Main, which allows the user to choose which axis to tune and the method (manual or automatic). The Manual option was used for tuning the NPADS robotic arms. The middle three pages provide tools for generating a Step Response, Trajectory, and Bode plot for a given set of parameters. The final page, Control Loop, allows the user to vary the value of the PID control gains for the motion control system on the given axis. Changing the values of the proportional gain (Kp), derivative gain (Kd), integral gain (Ki), and derivative sampling period (Td) provide various, often unstable, results during the iterative process of servo tuning. Following the instructions provided by National Instruments' online support center [Ref 10] for manually tuning a motor, all six joint motors were tested and categorized. Figure 24 shows the interactive Control Loop page used to manually adjust the PID control parameters. Appendix C provides the calculated gains.

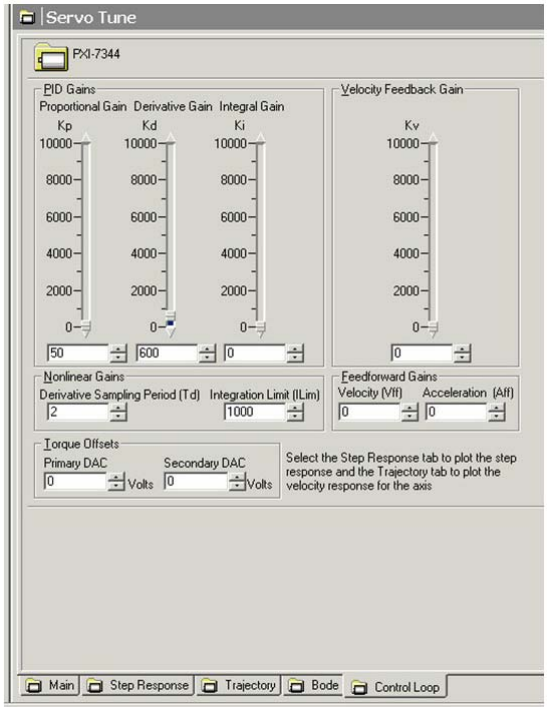

Figure 24 MAX Servo Tune Control Loop Page

Following motor tuning, the aforementioned 1-D interactive module of MAX allowed preliminary testing of the joints individually to ensure proper performance. This

testing proved 360 degree motion, velocity control, positional control, encoder operation and verified encoder count for the output shaft as 400,000 counts per revolution for the shoulder motors and 200,000 counts per revolution for the elbow/wrist motors (the difference is due to the gear ratio of the two models).

Finally, the most important application of MAX is that once all of the settings are properly defined and the motors are tuned, MAX saves the data to a configuration file unique to the controller. Therefore, when control programs, such as the ones that follow, are written, the configuration file can be called via a FlexMotion icon that will initialize the 7344 Motion Control card to the parameters saved in that file. Each time the system is powered down, the controller must be initialized prior to operation of the robotic arms.

C. COMBINED CONTROL

1. Combined Control Code Interface

The MAX 1-D interactive module provided an important tool in testing operability of the joints individually, but a 3-D control program was needed to fully flex the controller to ensure that multi-joint operations were feasible. The design philosophy behind the manual control program focused on creating a real-time command-in, desired outcome-out system with relatively user-friendly control implementation. LabVIEW, as stated previously, is a graphical programming language. A LabVIEW program consists of two parts: a diagram, which is a graphical illustration of the program flow, and a front panel, which forms the I/O (input-output) interface between the user and the program. Built into the language is the ability to readily create controls (such as knobs and slide bars) and indicators (such as dials and digital readouts) on the front panel, corresponding to functions on the diagram, to facilitate use of a program. Capitalizing on these built-in functions and for simplicity of testing and demonstration, both the manual control program and the subsequent autonomous control programs are built into one diagram and front panel. Figure 25 shows the appearance of the full control program front panel. The Emergency Stop switch (top left) and the Joint Velocity and Position indicators (top right) are shared by all sub-programs.

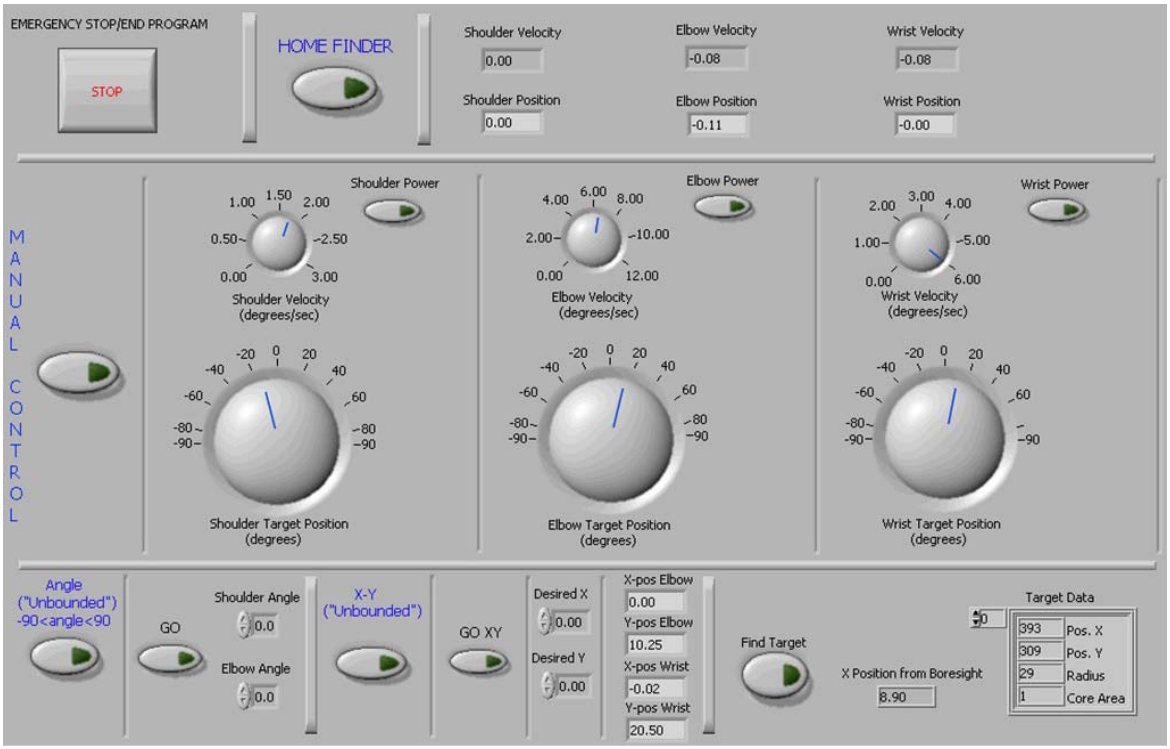

Figure 25 NPADS Robotic Arm Manual/Autonomous Controls Front Panel

2. Combined Control Code

As stated in the previous section, both the manual and autonomous control codes are part of a single program. Figure 26, Figure 27, and Figure 28, on the following pages, show the LabVIEW diagram in its entirety. The rectangular structures in the diagram represent loops or subroutines of various types. The outer rectangle is a while loop that allows the code to continue operation as long as the Emergency Stop routine is not activated. The inner loops of the Control Code diagram, from top to bottom, are the Home Finder subroutine, Manual Control subroutine, Commanded Angle subroutine, Commanded X-Y subroutine, and Visual Target Acquisition subroutine. These subroutines are discussed in detail later in this chapter.

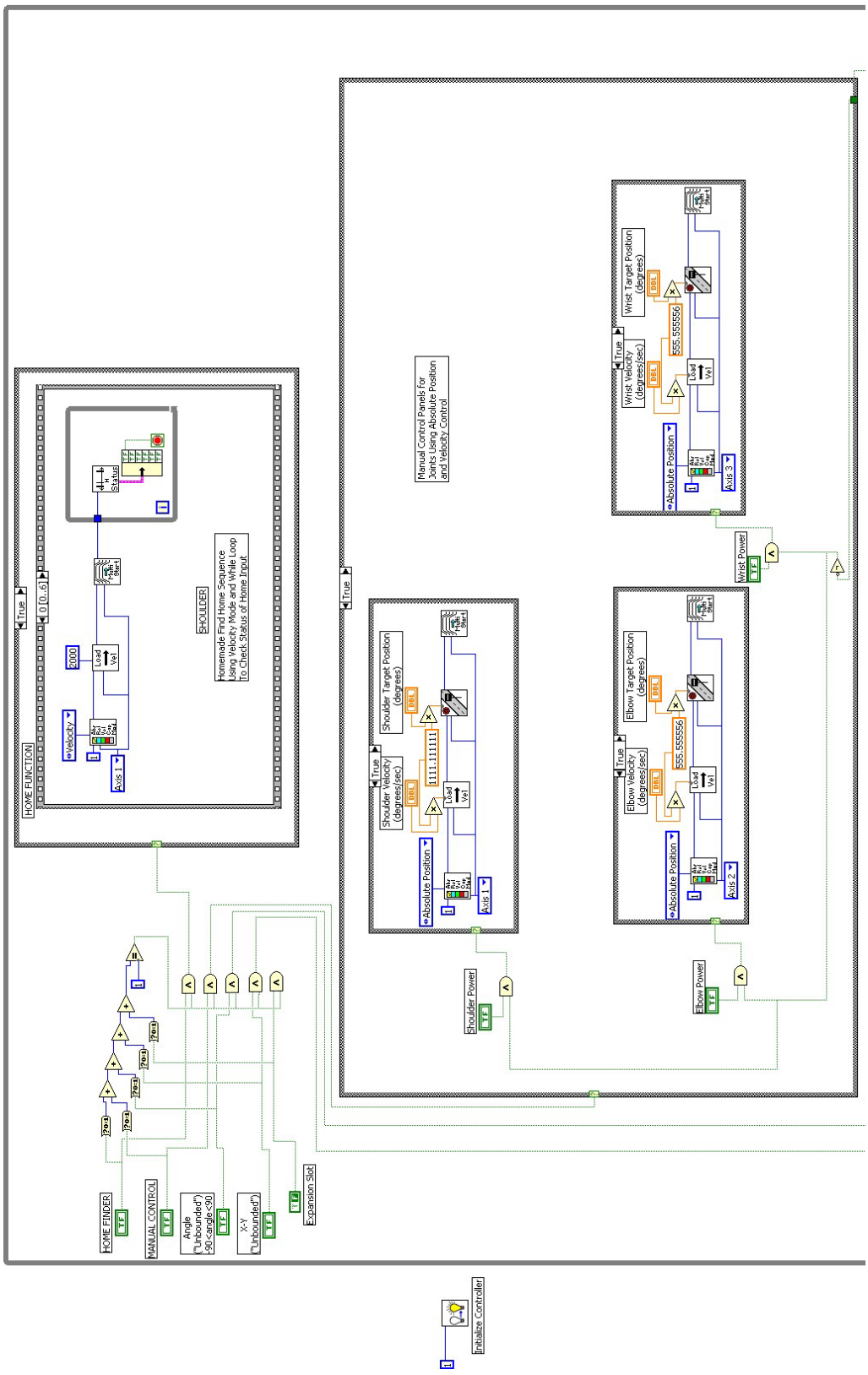

Figure 26 LabVIEW Control Code Diagram – Part 1 of 3

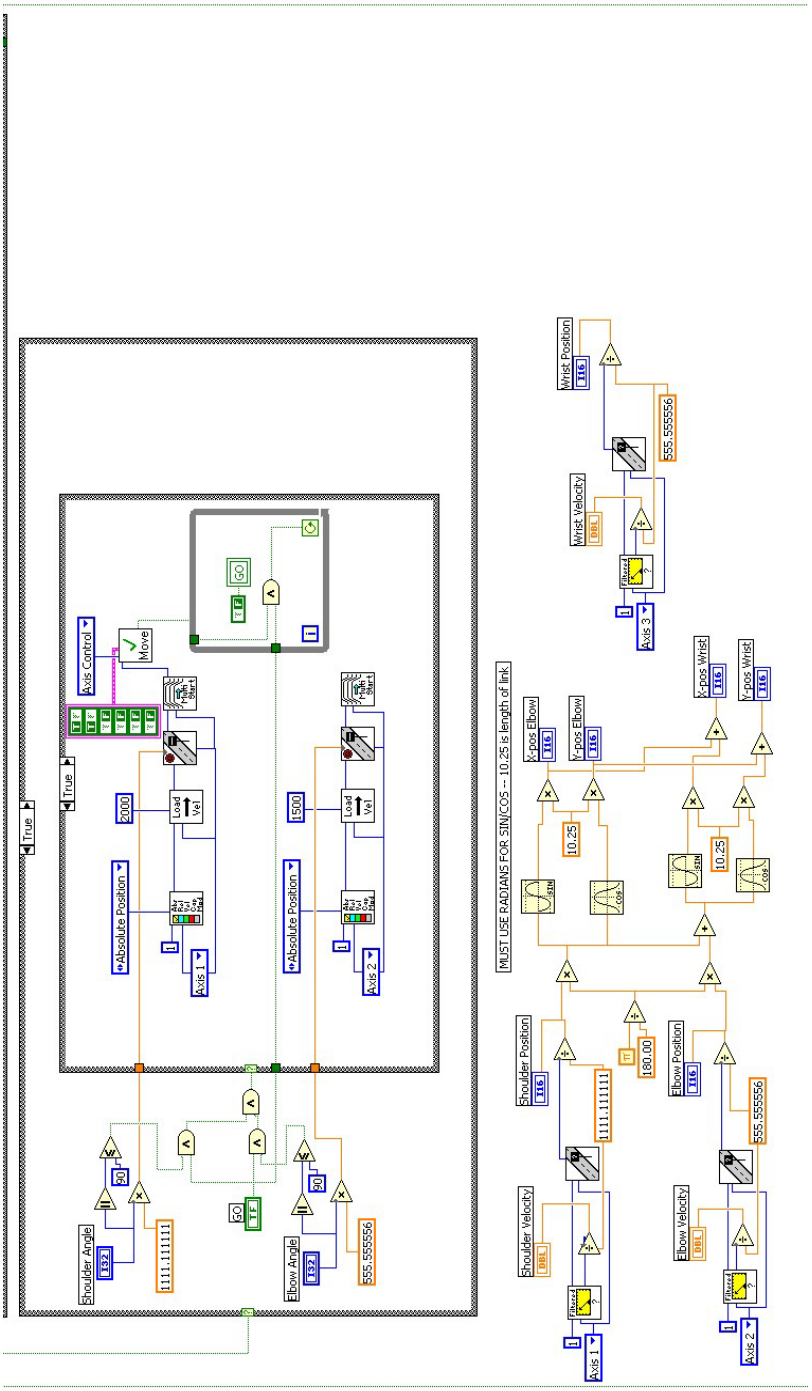

Figure 27 LabVIEW Control Code Diagram – Part 2 of 3

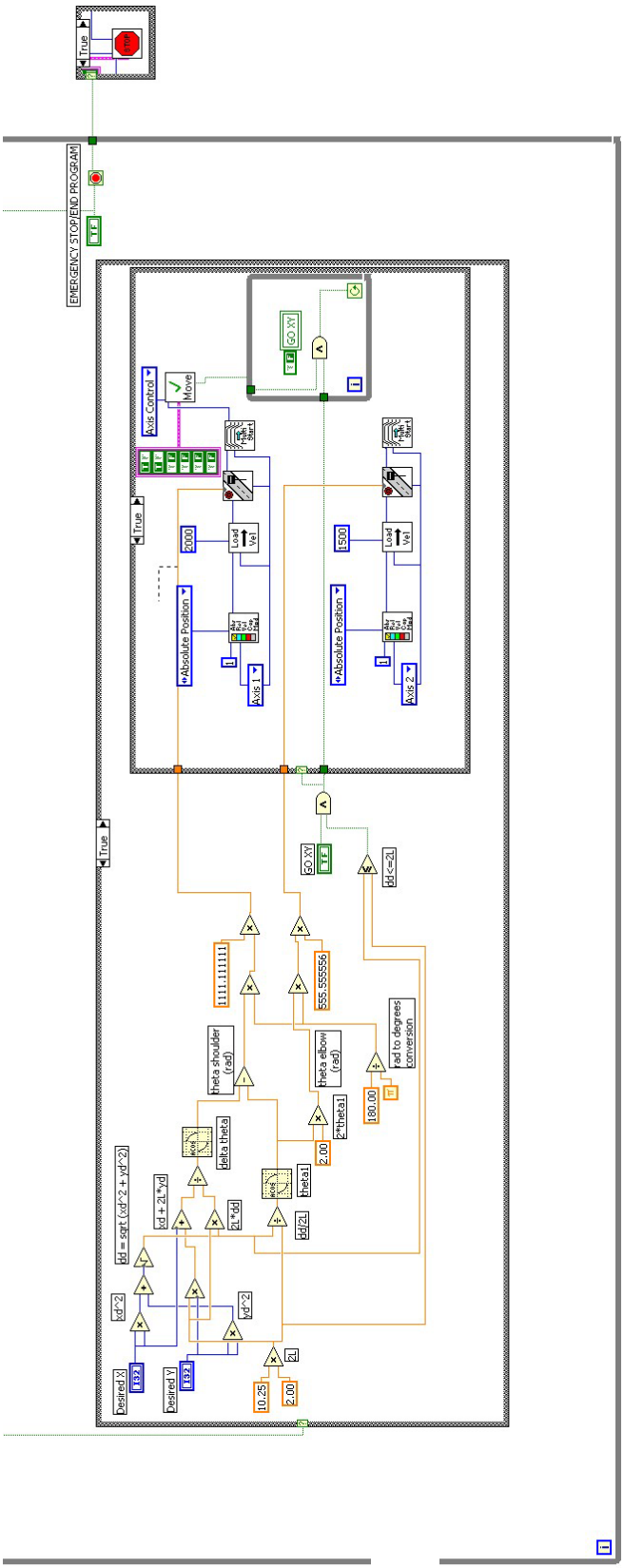

Figure 28 LabVIEW Control Code Diagram – Part 3 of 3

The Emergency Stop routine, displayed in Figure 29, checks for an input from the Emergency Stop button on the front panel (represented by the T F box wired from the left, in the diagram) and uses the Case structure (rectangular frame) to determine the necessary operations. If the signal is false (no input), the main While loop continues running and the Stop routine continues monitoring the signal for input; if true (input), the main While loop discontinues and all motors on the appropriate control card are sent a Kill command to disable power flow, stopping the motors. This feature was implemented for safety during testing. When the program is stopped, the motors are sent a Kill command as well.

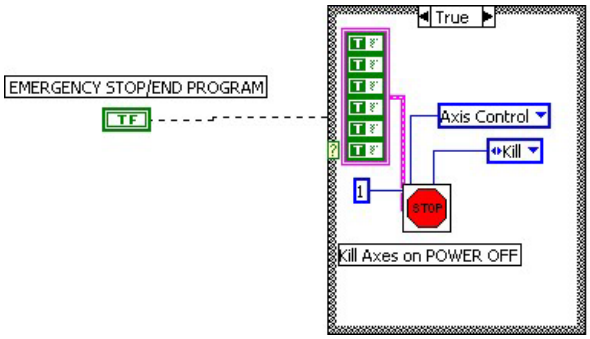

Figure 29 Emergency Stop Routine Code

Another item of note is the Initialize Controller routine on the left side of the diagram, outside the while loop. This routine (Figure 30) is a FlexMotion Virtual Instrument (VI), a subroutine or command provided with the software suite, that reads the current motion control configuration file developed using Measurement & Automation Explorer, as mentioned in the section on Motor Tuning. The constant (number) wired to the icon identifies which 7344 Motion Controller is to be loaded with the configuration file. This routine commences upon program initiation.

Figure 30 Initialize Controller Routine Code

After controller initialization, the main While loop is entered and the code waits for a functional selection by the user. The front panel master switches discussed earlier control this selection. To ensure that the motion control system receives commands from a single subroutine at a given time, the Boolean mechanism illustrated in Figure 31 uses a series of comparisons (Boolean gates) to verify that only one function is chosen. The dashed lines represent the command lines connected to the various subroutine loop structures.

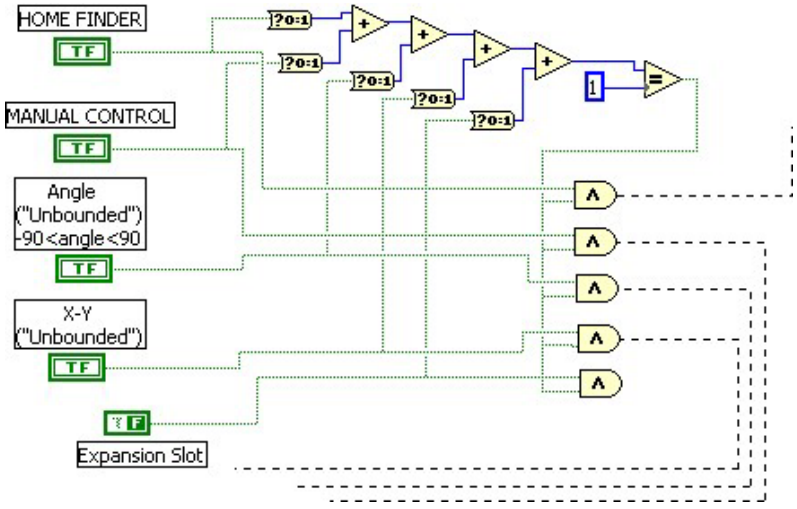

Figure 31 Switching Mechanism Code

Finally, Figure 32 shows the code providing output to the indicators on the front panel. For each joint, calculations are completed based on encoder feedback signals and the motor parameters (i.e., counts per revolution) to provide instantaneous motor velocity, motor position relative to the reference-zero, and (x,y) position for the elbow and wrist joints. This figure illustrates the ease of integration between FlexMotion VIs (i.e., "FILTERED" gauge, which reads encoder signals for velocity, and the road icon, which reads position) and standard LabVIEW VIs (i.e., trigonometric functions and mathematical expressions). This algorithm runs independent of any of the other subroutines – outputs are provided continuously following controller initialization.

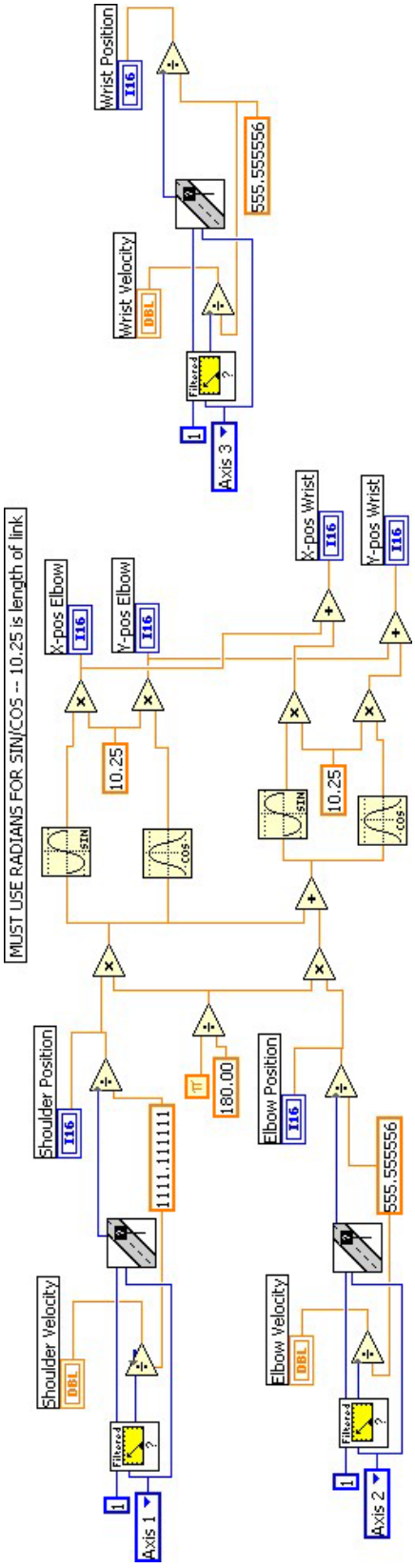

Figure 32 Position and Velocity Indicator Code

D. MANUAL CONTROL

3. Manual Control Interface

Figure 33, below, provides a closer look at the Manual Control program front panel. To operate in Manual Control mode, the switch on the left must be toggled on and left in that position, with none of the other master switched triggered. The switches for Shoulder Power, Elbow Power, and Wrist Power are isolation switches that will allow for 1-D, 2-D, or 3-D operation. Each axis has two dials for control of absolute velocity and desired position. As stated earlier, this program was designed to run real-time such that the velocity control acts as a throttle, setting the instantaneous velocity of the joint, and the position control acts as a steering wheel; in other words, the joint does not have to reach the previous input (velocity or position) before adjusting to a new command.

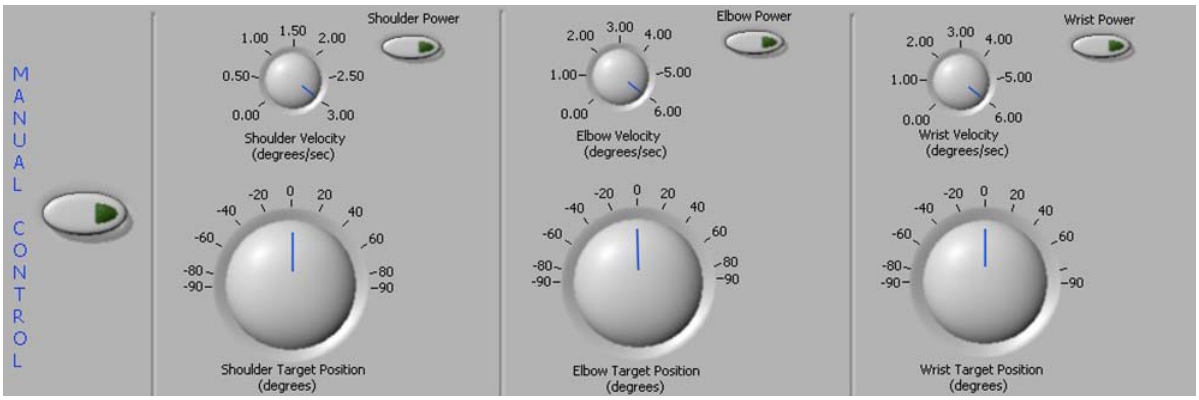

Figure 33 Manual Control Front Panel

4. Manual Control Code

The Manual Control code (Figure 34) consists of a set of nested Case Structures. The code is initiated upon a True input to the outer Case and a False input from the Emergency Stop button. If either of these inputs switch, motion will cease. The three T-F isolation inputs (from the front panel switches) for Shoulder, Elbow, and Wrist Power initiate entry into the inner Case structures.

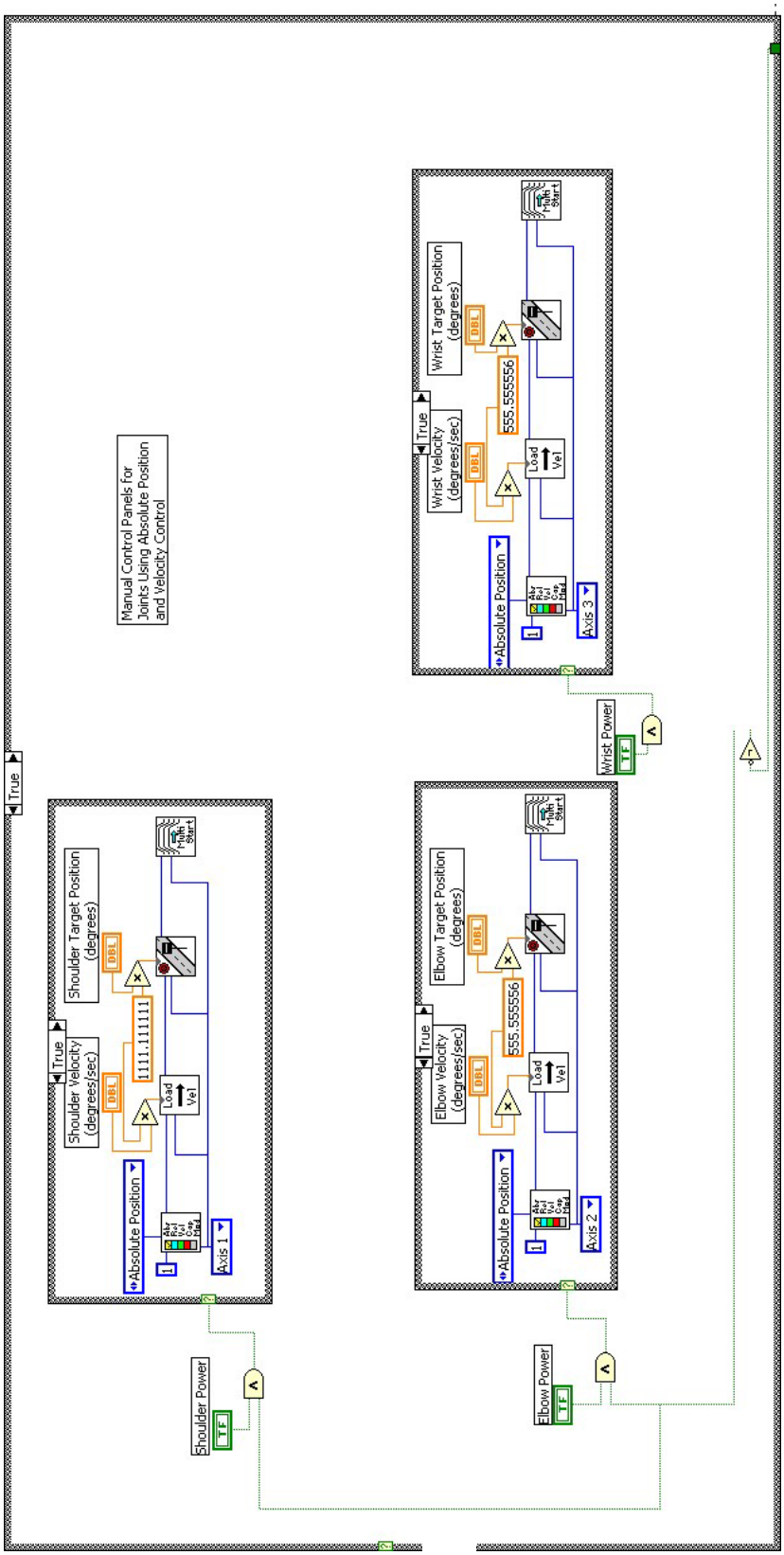

Figure 34 Manual Control Code

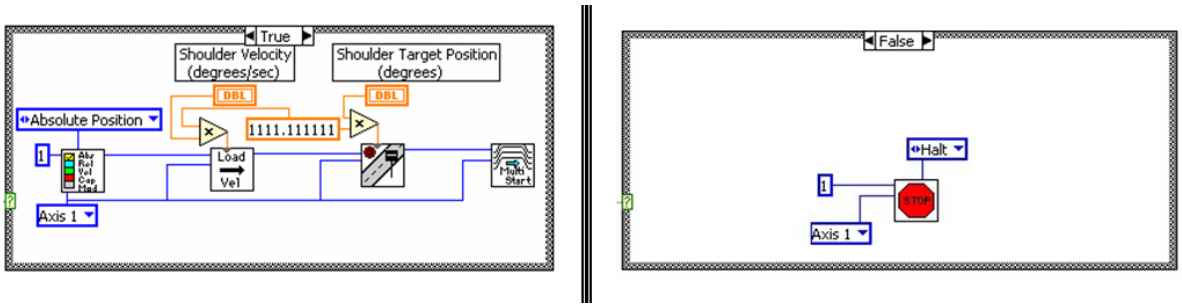

Figure 35 Joint Operation/Isolation Code

Figure 35 provides the two paths within the inner Cases. If the joint power switch is ON, the True case (left) is initiated and the user will experience real-time control of the joint using the front panel controls for velocity and position. These controls are restrained to +/- 90 degrees in position (all joints) and 3 degrees per second (shoulders) or 6 degrees per second (elbows and wrists) in velocity for better control and safety. The code uses FlexMotion's Absolute Position mode with variable inputs to the Load Position and Load Velocity VIs to create instantaneous control. Since a Case structure is used, as long as the switches remain True, the functions inside the structure will continue to run.

If the joint power switch is OFF, the False case (right) is initiated and the joint is given a Halt command (the motor still receives power from the amplifier to hold position) using the Stop Motion VI. As long as the Manual Control master switch remains ON and the Emergency Stop signal remains False, the isolation switches can be turned ON and OFF at will to provide simultaneous control of the desired number of joints.

E. AUTONOMOUS CONTROL

A single autonomous control algorithm was not created in the course of this thesis. Rather, a set of four autonomous subroutines were designed to provide for autonomous functionality of the robotic arms when integrated with the NPADS vehicle control program. These subroutines provide tools aimed at autonomy and various approaches to interaction with a vehicle based targeting architecture. The design philosophy focused on generating a set of algorithms that could be commanded by

various inputs, thus facilitating flexibility in control system integration at such time that the arms are mated permanently with the vehicle.

The autonomous subroutines are meant for implementation into a governing control program, namely that of the NPADS vehicle. Each subroutine provides a segment of the autonomous control loop: self-knowledge, targeting, and control. Figure 36 provides a basic schematic of the robotic arm control scheme and identifies the subroutine associated with each function [Ref. 11]. The figure shows that tuning the motors provides the PID gain inputs to the control system and the subroutines described in the following sections supply the three components listed above, creating a standard closed-loop control system.

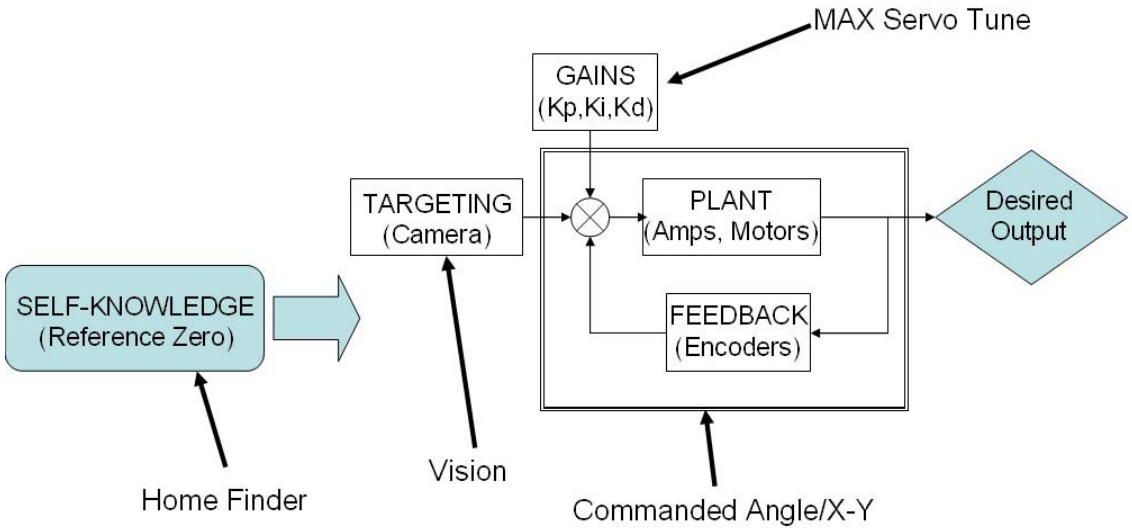

Figure 36 Autonomous Control System Block Diagram

1. Home Finder

a. Home Finder Interface

The first step in the process of autonomy involved devising a method to provide an accurate, repeatable reference point at power up, such that the joint has knowledge of its position at all times. As stated in the previous chapter, the joint motors are equipped with an optical encoder that includes an Index mark. LabVIEW's FlexMotion module includes a Find Index subroutine and, ideally, the Index would be

used as the reference point; however, since the encoder is situated on the drive shaft, prior to the gearing, the Index is found multiple times per revolution of the output shaft, the number of times being determined by the gear ratio. For an application where the motors were turning many revolutions, the Index would be a useful tool; but, joint motion of the arms is restricted to less than one revolution, which makes the Index signal useless since a dependable, repeatable instance is unlikely.

To alleviate this problem, using FlexMotion tools, a new subroutine was created to be run only at power-up to find and set a reference position. To ensure repeatability, the momentary switches mentioned in Chapter II were situated on the shoulder and elbow joints such that when the arms are in a stowed configuration, the inter-joint linkages would make contact with the switches. This subroutine causes the joint motors, one at a time, to move toward their respective home switch until contact is made. Once the computer receives the signal that Home is found, the position can be set to a MAX-defined value, whether zero or some other location. This feature and more details of the code are provided in the next section. Figure 37 shows the Home Finder trigger on the front panel, alongside the three joint position and velocity indicators (velocity is provided in degrees per second and position in degrees).

Figure 37 Home Finder Trigger with Velocity and Position Indicators

b. Home Finder Code

As with the Manual Control Code described above, and all of the following autonomous subroutines, the Home Finder code is built inside a Case structure to enable use of the Boolean switch. Within the Case Structure lies a Sequence structure, having the appearance of a film frame, which allows a sequence of operations to be carried out one at a time. There are seven frames to this sequence: two for each joint and one frame to end the subroutine. Figure 38 shows the two frames required to find the reference position for the right shoulder joint. The frame on the left utilizes FlexMotion

Velocity control, with a constant input to the Load Velocity VI causing the shoulder joint motor to continue moving clockwise (positive direction) until the momentary switch triggers that Home is found. The While loop on the right side of the left frame causes a continuous query of the Home Input, checking for contact. Once contact is verified, the motor is stopped and the Sequence moves to the next frame (Figure 38, right) where the Reset Position VI renames the current position to the position desired. Table 3 lists the stowed positions for the shoulder and elbow joints of the two arms. Though the algorithm included code for the wrist, the wrist joints have been ignored until such time as there is a manipulator or grapple mechanism installed so that the switches can be placed appropriately.

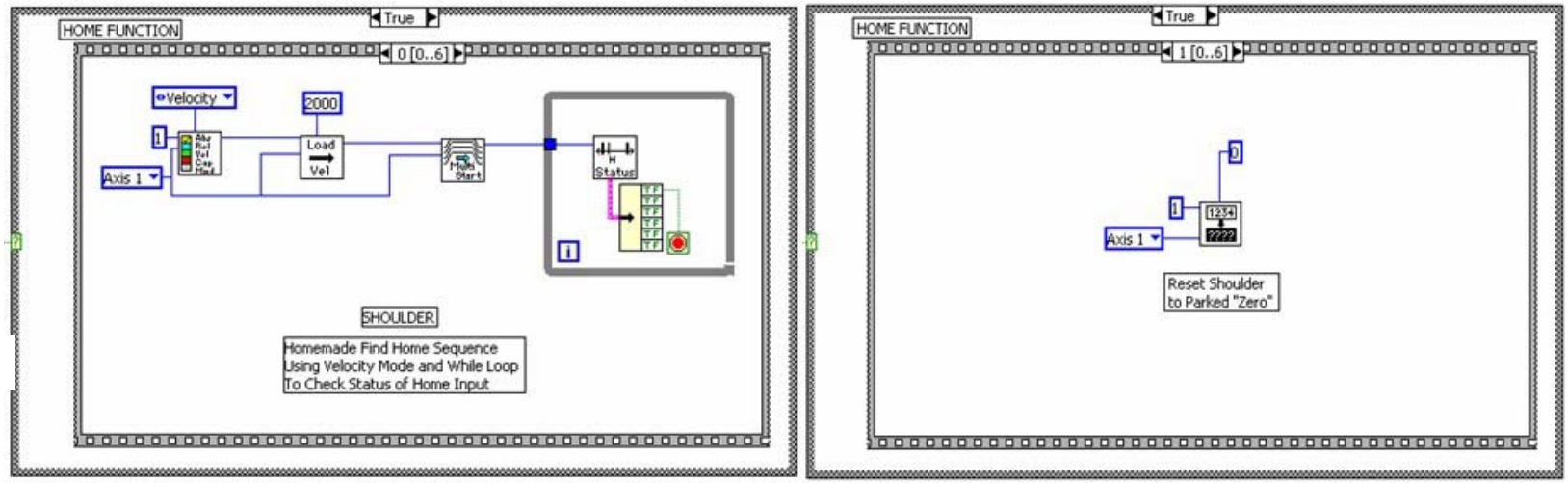

Figure 38 Home Finder Code (2 Frames)

Table 3 Desired Home Positions

LEFT ARM	
Shoulder	-172,500 counts
Elbow	+65,750 counts
RIGHT ARM	
Shoulder	+175,500 counts
Elbow	-65,750 counts

The final frame of the sequence, displayed in Figure 39, provides a means to end the Home Finder function. The Master Switch is created as a Local Variable and when the subroutine has completed the sequence and gets to this frame, the master switch is tripped to the OFF position. For implementation in the NPADS control code, this frame can be used to change a reference bit such that the algorithm is recognized as complete.

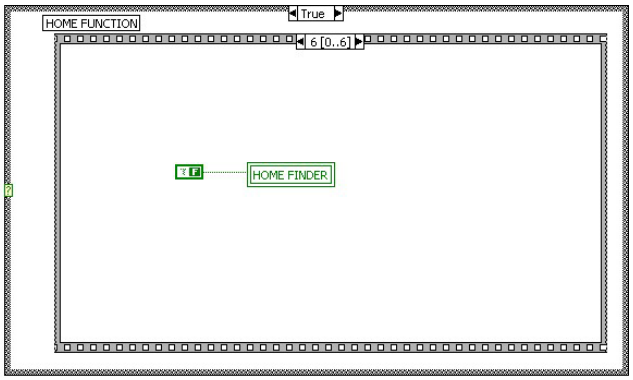

Figure 39 Home Finder Code (Final Frame)

2. Commanded Angle

a. Commanded Angle Interface

Once the initial position of the joints are known, a method for commanding the arm must be defined. The first approach designed fed directly from the Manual Control program: angular commands. The front panel, shown in Figure 40, is a system of a master switch, two commanded angle digital controls, and a send command switch. Once the master switch is triggered, the user utilizes the two digital controls to provide desired absolute angular positions for the shoulder and elbow joints; then, depressing the GO button sends the command to the controller. The desired angles must

be input in reference to the particular joint reference-zero as defined at power-up, ideally set at what would be thought of as "forward" relative to the joint motor (see Figure 41). The joint motors will proceed to the desired positions at a constant velocity as specified within the subroutine code.

Figure 40 Angle Command Front Panel

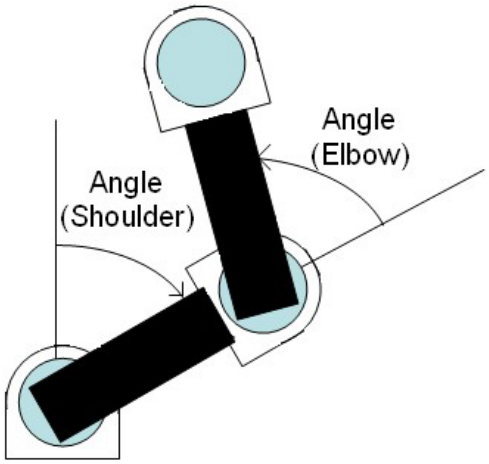

Figure 41 Robotic Arm Angular Coordinate Frame

b. Commanded Angle Code

Once the Commanded Angle master switch is set to the ON position, the code displayed in Figure 42 begins to run. The inputs from the shoulder and elbow digital controls, which the user utilizes to enter desired angles in degrees, is simultaneously converted into the proper position in counts for each of the motors and checked to ensure that the desired position is within the +/- 90 degree constraints. If either of the desired angles are outside the constraints or the GO button has not been triggered, the inner False case (Figure 43) is implemented which simply maintains the GO switch in the OFF position; as with the Home Finder code, the GO switch is a local

variable. Once the desired angles are verified and the GO button is triggered ON, the inner Case structure is entered for the True case. Motion is initiated using FlexMotion Absolute Position mode with a constant velocity input to the Load Velocity VIs and the Load Position VIs being fed by the converted positions mentioned earlier. The Move Complete VI checks both axes to verify that the commanded angles have been reached for both the elbow and shoulder. Once motion is complete, the While loop on the right is entered and switches the GO switch to the OFF position, ending operation of the case.

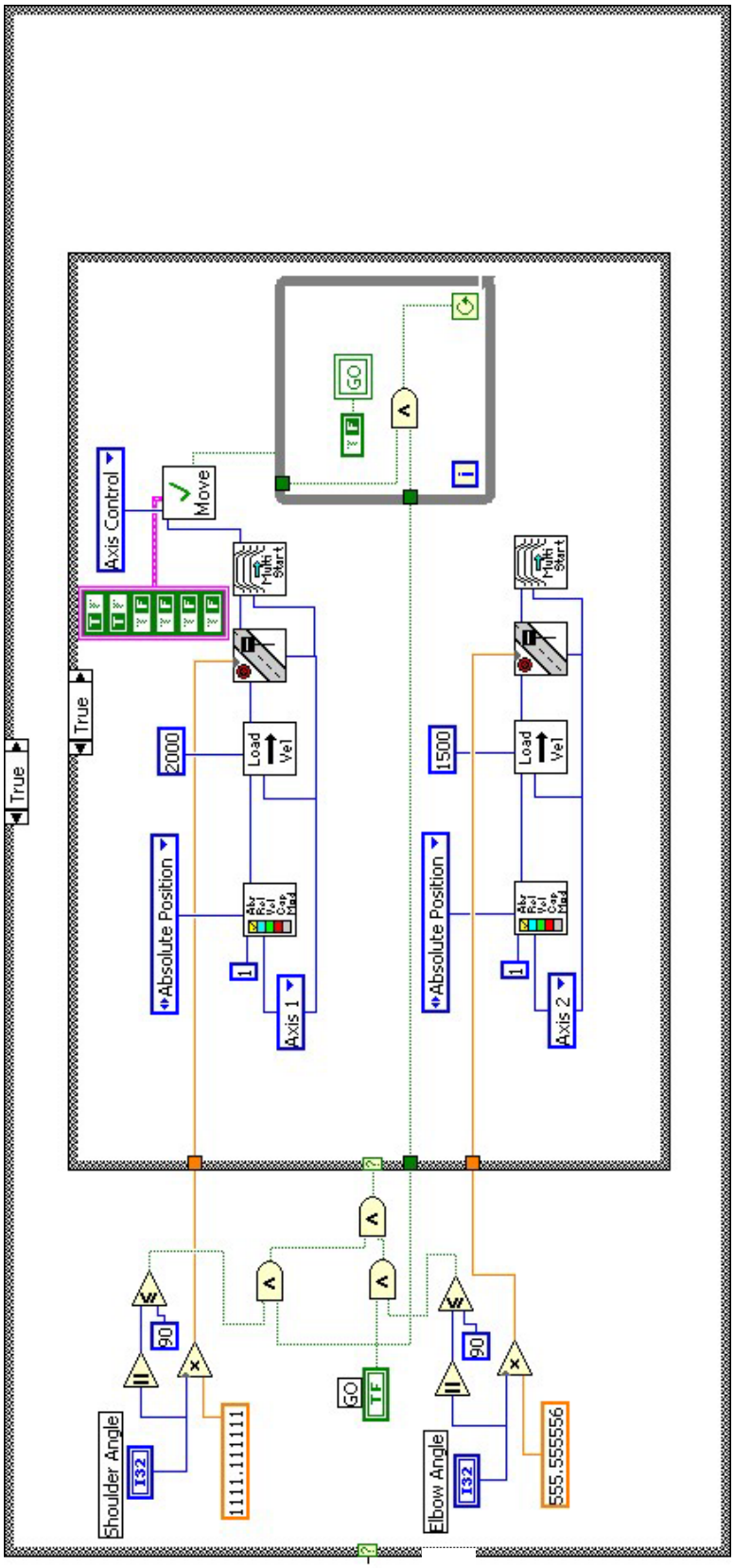

Figure 42 Commanded Angle Code (True Inner Case)

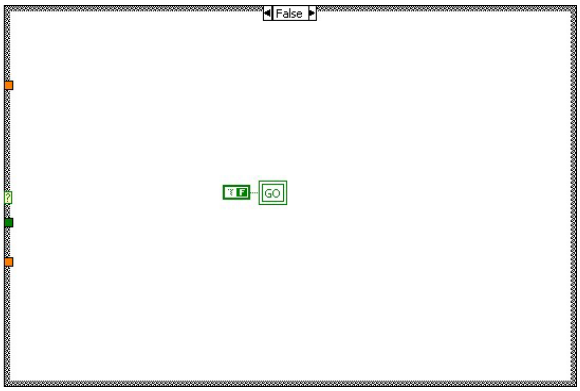

Figure 43 Commanded Angle Code (False Inner Case)

3. Commanded X-Y

a. Commanded X-Y Interface

The second approach is derived from the initial control algorithm used by the NPADS vehicle to identify its position on the granite table: x-y commands [see Ref. 4]. Figure 44 illustrates the X-Y Command front panel, which includes the same basic user controls as the previous subroutine as well as x and y position indicators for the centers of the elbow and wrist joints (in inches). Figure 45 describes the robotic arm coordinate system used for this algorithm. The (0,0) point is set as the center of the shoulder joint hollow shaft. Again, the user sets the Desired X and Desired Y digital controls for desired wrist joint position, then presses the GO XY button to initiate motion. As above, the arm joints are driven at a constant velocity set in the program code to the user-defined wrist position. Due to the length of the arm, wrist position is limited to positions within a semi-circle having a radius of 20.5 inches (0.52 m).

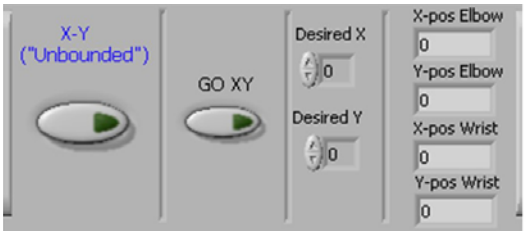

Figure 44 X-Y Command Front Panel

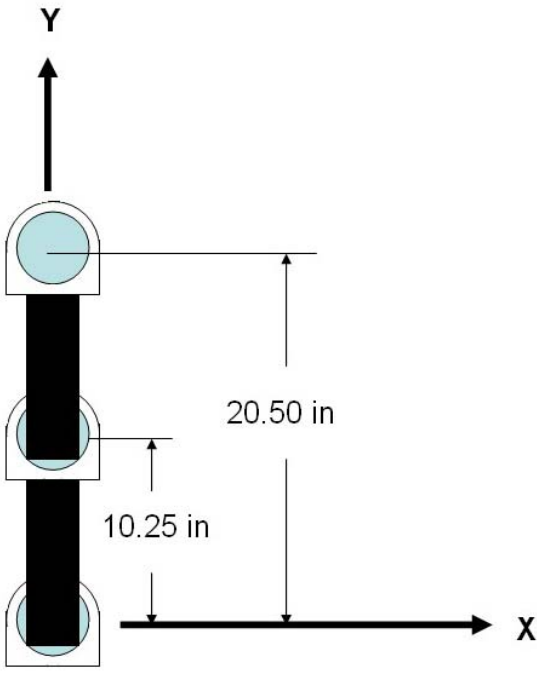

Figure 45 Robotic Arm X-Y Coordinate Frame

b. Commanded X-Y Code

Upon initiation of this subroutine using the Commanded X-Y master switch, the user utilizes the digital controls to input the desired x and y position of the center of the wrist joint in inches; for example, if the user desired the arm to be positioned straight out, the desired position would equate to x = 0, y = 20.5 or (0, 20.5). Prior to motion initiation, the desired coordinates proceed through a series of algebraic and trigonometric functions to convert the x-y position, first, to a set of angles and then, finally, to a pair of encoder counts. Once the position is verified to fall within the aforementioned semi-circle and the GO XY switch has been triggered, the inner Case structure is entered, which functions exactly as the one described for the Commanded Angle code. The False case works exactly the same, as well, restricting the GO XY switch to achievable desired positions. Figure 46 provides the code for this subroutine.

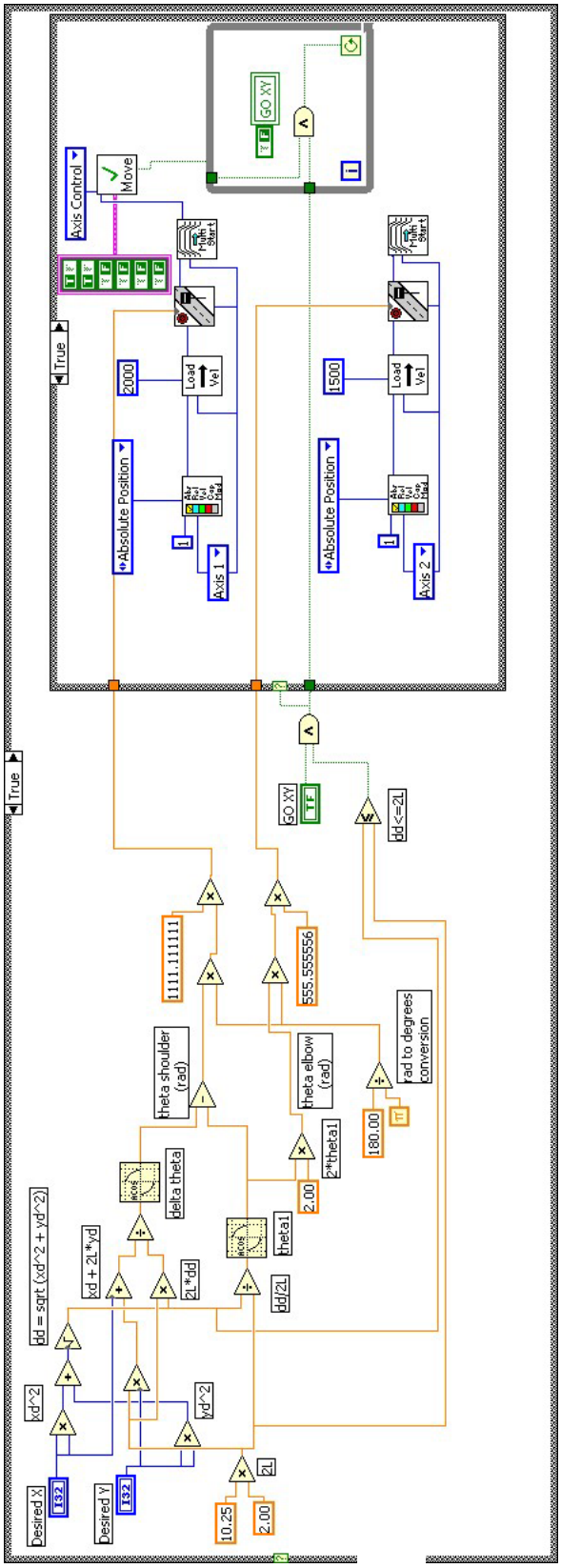

Figure 46 Commanded X-Y Code

4. Visual Target Acquisition

a. Visual Target Acquisition Interface

The previous two subroutines, though autonomous in operation, require an external input, whether from a telerobotic user or an output from the NPADS onboard control program. In order to create a fully autonomous control algorithm for the arms, an integrated sensor was required for target detection. The bullet camera described in the previous chapter was chosen as this sensor. Using an algorithm similar to that of the NPADS vehicle, it is possible to isolate the x-position of a target. The front panel for this algorithm provides only a function ON/OFF switch, an indicator expressing x-position of the target in relation to the wrist camera centerline (in inches), and a raw data output from the image acquisition software (in pixels). The Visual Target Acquisition algorithm may be started and stopped at any point as it is independent of the switching routine described above. Figure 47 shows the Visual Target Acquisition user control and indicators.

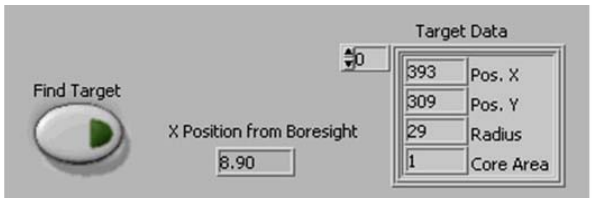

Figure 47 Visual Target Acquisition Front Panel

Using only one camera, it is impossible to determine distance (y-position) from the arm; however, it is believed that once the targeting camera on the NPADS vehicle is implemented [see Ref. 4], it will be possible to determine y-position of the target using both cameras and an algorithm similar to a nautical running fix. The lack of depth perception makes it difficult to localize even the lateral x-position since the field of view of the camera is dependent on the distance between the camera and the target. This algorithm is designed for operation on the test harness, where the distance falls within a fixed range. The rudimentary target consists of a single black circle, just over 6 inches in diameter.

Use of the vision system is only in its infancy as part of this thesis. Implementation occurred in order to prove the ability to operate a vision system and

motion control system concurrently and to provide support for future growth. The only degradation experienced operating the systems simultaneously occurred with the front panel indicators. When the vision system is running, the position and velocity indicator update rate is slowed significantly.

b. Visual Target Acquisition Code

LabVIEW's Image Acquisition (IMAQ) Module and Image Builder were used to construct the algorithm shown in Figure 48. Unlike the previous subroutines, this code was developed to run concurrent with any of the other functions; therefore the Boolean Find Target switch is not wired through the switching mechanism discussed earlier. Once the master switch is turned ON, the Case structure is entered and image acquisition begins and continues until the switch is triggered OFF. A snapshot, or single image, is captured from the bullet camera mounted on the wrist of the left arm. Using IMAQ tools, the snapshot is filtered of clutter and edge noise. The new image is then further filtered to identify circular structures that fall in a set range of diameters. The range is specific to the distance expected while the arm is mounted to the test harness. Once the circle has been identified, the VI outputs raw Target Data in pixels, which is sent to the front panel. The Target Data includes circle center x (horizontal) and y (vertical) position in pixels from the upper left corner of the image, the radius of the circle in pixels, and the core area which comes from a set algorithm in the VI. The raw x-position is then converted into the x-position from the center of the camera (center of the wrist joint) in inches. The image is 680 pixels wide, so the raw position is subtracted from the halfway point and then converted to inches using a pixels per inch conversion factor. This conversion factor is determined by the proximity of the target, but is set in the code for test harness operation. The code will continue to output target position as long as the target is visible to the camera and the master switch is ON.

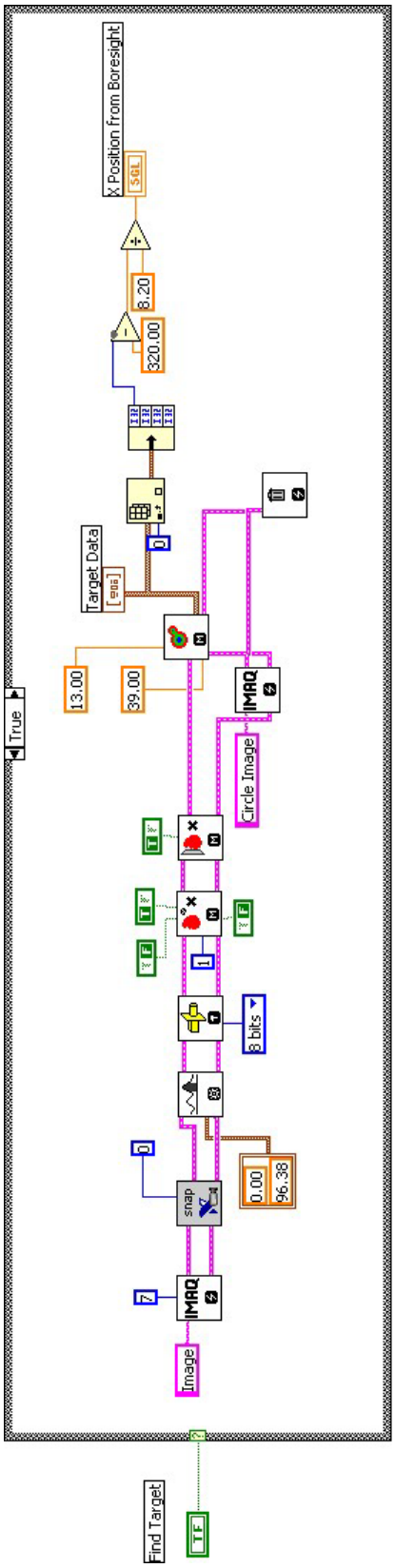

Figure 48 Visual Target Acquisition Code

THIS PAGE INTENTIONALLY LEFT BLANK

IV. OPERATION AND PERFORMANCE

Nearly all testing and operation of the robotic arms was conducted using the test harness, in order to minimize risk to the NPADS vehicle and to provide independent testing of the arms during the concurrent development of the vehicle main body. This chapter describes the procedures utilized during this thesis for operation of the robotic arms and provides performance data for the subroutines described in the previous chapter. Though the majority of arm operations occurred on the test stand, a brief explanation of the operational procedures for an arm joined to the NPADS vehicle is provided as well.

A. ROBOTIC ARM OPERATION

As with testing of all powered equipment, there are procedures for start-up, operation, and shutdown of the robotic arm and its associated equipment. The following sections describe the initial setup of the robotic arm, on the test stand and the main body, as well as these procedures.

1. Robotic Arm Test Setup

The robotic arm components used during operation on the test harness are exactly the same as those used when the arm attaches to the NPADS vehicle, with the exception of a smaller, AC-powered PXI computer (described in Chapter II). Figure 49 illustrates the location of the major components at the fixed base location. Not shown in the figure is the floatation air supply system, comprised of a thirteen cubic foot compressed air tank and two pressure regulators supplying 5-10 psi air to the air pads, located beneath the granite table directly below the test harness. To conserve battery life and to eliminate the need of a second set of DC-DC converters, three AC-powered DC power supplies are used to supply 5, 12, and 24 Volts to the various system components.

As mentioned previously, the zero position of the arm is with the two links aligned directly forward of the test harness as shown in Figure 50. This figure displays

also the connection of the shoulder motor housing to the test harness and the visual target located across the table from the arm.

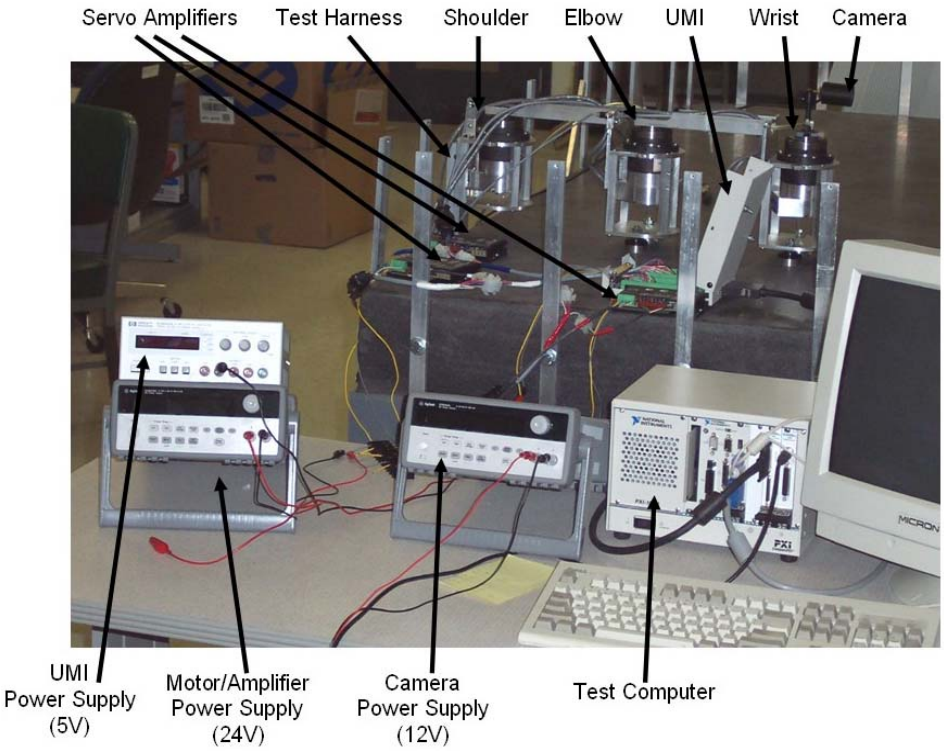

Figure 49 Robotic Arm Test Setup

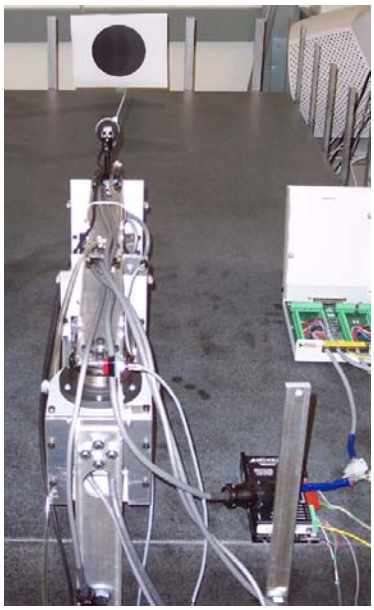

Figure 50 Test Harness Arrangement, Zero Reference Configuration

2. Robotic Arm Pre-Operation

In order to ensure safe, proper operation of the robotic arm while attached to the test harness, a sequence of tasks need to be performed prior to system operation. Adherence to these procedures ensures the safety of personnel and equipment as well as providing a systematic check of the robotic arm components. Table 4 lists the Pre-Operation procedures.

Table 4 Robotic Arm Pre-Operation Checklist

Action	Notes
1. Clean Granite Table	Use fine brush and Silicon spray
2. Check general condition of wiring and hoses	
3. Verify floatation tank full and pressure set correctly	Should provide 5-10 psi. Test by briefly turning on air.
4. Turn on Test Computer	No password required
5. Initialize PXI 7344 Motion Control Card	Open MAX>Devices and Interfaces>PXI-7344>Device Resources, press Initialize in Upper Left corner
6. Turn on UMI Power	5V Power Supply, verify connection
7. Turn on Motor/Amplifier Power	24V Power Supply, verify connections
8. Verify Amplifier LEDs light GREEN	Located next to MOLEX connector
9. Turn on Camera Power *(only if using Vision system*)	12 V Power Supply, verify connections
10. Turn on floatation air	
11. Test for positive control of all three joints	Use MAX>Devices and Interfaces>PXI-7344 >Interactive>1D Interactive. Use Velocity control at low speed (1000-2000 counts/s), press Apply and then Start choosing one joint at a time to verify control and feedback. Use KILL to stop motion.
12. Align arm to Zero Reference Configuration	Use 1D interactive to maneuver joints such that they align as in Figure 50. As each joint is positioned correctly, press Reset Position and the joint position will be set to zero.

WARNING: If the feedback system is not initialized properly or feedback signals are lost for some reason, the joint WILL move, but at a faster velocity than anticipated. Be ready to initiate KILL to stop motion. If initialization is incorrect, reset the motion control card (see Post-Operation procedures), disconnect power to all components, reboot the test computer, and begin the Pre-Operation procedures again.

3. Robotic Arm Operation

Once the Pre-Operation checklist is completed, the robotic arm is ready for operation using the Combined Control program described in the last Chapter. On the test

harness, commands are sent from the test computer through the Motion Control Card to the UMI for redistribution to the motion control components.

If the arm is integrated with the main body, there are two modes of operation available. If the computer peripherals (i.e., mouse, keyboard, and monitor) are connected to the NPADS control computer, the Combined Control program data flow will act just as it would on the test harness. If the NPADS vehicle is wireless, however, the robotic arm control program must follow Data Socket initialization procedures [Ref. 4] such that an offboard DAQ computer can act as a command terminal to upload commands via the wireless Ethernet. Wireless operation of the Manual Control code was verified briefly through testing, but only to prove the capability.

4. Robotic Arm Post-Operation

In order to conserve consumables and ensure that the system is ready for follow-on operations, a series of Post-Operation procedures are required to shut down the system. Table 5 lists the steps required following robotic arm operation.

Table 5 Robotic Arm Post-Operation Checklist

Action	Notes
1. Align arm at safe position	Using either Manual Control or MAX 1D Interactive, move the arm to a position on the table appropriate for stowage.
2. Exit Control Program	*If not already done*
3. KILL all axes	Use MAX 1D Interactive to KILL the Shoulder, Elbow, and Wrist joints
4. Turn off floatation air	Refill tank, if necessary
5. Turn off Camera Power *(if used)*	
6. Turn off Motor/Amplifier Power	Open MAX>Devices and Interfaces>PXI-7344>Device Resources, press Initialize in Upper Left corner
7. Turn off UMI Power	5V Power Supply, verify connection
8. Reset 7344 Motion Control Card	Use MAX>Devices and Interfaces>PXI-7344 (Status Page), press Reset Device, ensure that controller shows Power Up Reset.
9. Shut Down Test Computer	Use Windows START menu to Shut Down the computer and turn off power when prompted.
10. Check general condition of wiring and hoses	

WARNING: If the system is not shut down in order, inadvertent motion at system start-up may result.

5. Robotic Arm NPADS Integration Setup

For integration onto the NPADS main body, the robotic arm shoulder joint is mounted to the wing of the vehicle base plate. Figure 51 provides the location of the major components of the motion control system.

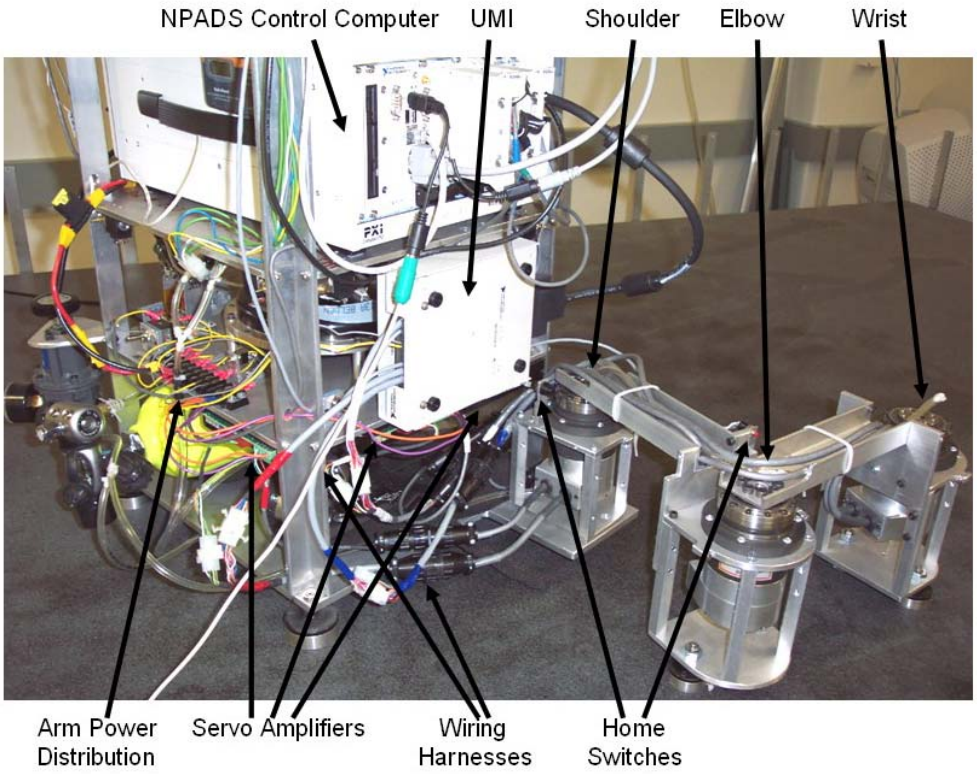

Figure 51 Robotic Arm NPADS Main Body Integration Setup

Though the majority of the Pre- and Post-Operation procedures are the same as when the arm is connected to the test harness, there are several additional electrical features on the body mounted system to ensure user and equipment welfare. These isolation switches, mentioned in Chapter II, are shown in Figure 52 and the procedures for their use are listed in Table 6. The only switch not shown is the NPADS vehicle DC conversion plate switch which provides the 5V supply to the UMI Power Switch. This switch is located on the underside of the second shelf, on the left side (looking forward), directly above the reaction wheel [see Ref. 4]. The camera will be wired into the vehicle

power distribution center; therefore, power will be supplied when the DC conversion switch is turned on.

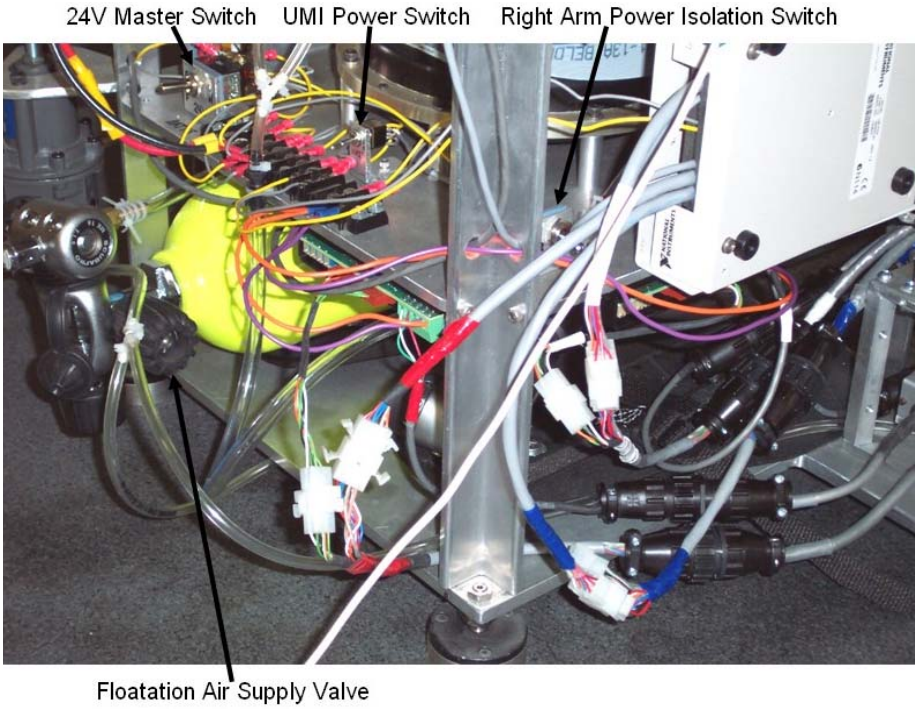

Figure 52 Robotic Arm Procedural Components on NPADS Vehicle

Table 6 Robotic Arm On-Vehicle Checklist Addendum

Pre-Operation	
Action	**Notes**
6a. Verify batteries are fully charged and connected	Two batteries in series should be above 21V
6b. Turn on DC conversion switch	
6c. Turn on UMI Power Switch	
7a. Turn on 24V Master Switch	
7b. Turn on Arm Power Isolation Switch(es)	
Post-Operation	
Action	**Notes**
6a. Turn off Arm Power Isolation Switch(es)	
6b. Turn off 24V Master Switch	
7a. Turn off UMI Power Switch	
7b. Turn off DC conversion switch	
7c. Charge batteries, if necessary	Two batteries in series should be above 21V

WARNING: If the system is not isolated properly, inadvertent damage or injury could result.

B. ROBOTIC ARM PERFORMANCE

The control algorithms developed for the robotic arms, described in the previous Chapter, were each tested to ensure that acceptable performance standards were met. The grading criteria included precision of joint movement versus commanded input and system response speed. The following sections will illustrate the results of these tests, in which all of the subroutines proved highly reliable. This performance analysis also served to verify the PID system gains derived from the tuning of the motor through the Measurement & Automation Explorer.

1. Manual Control Performance

The first software to be tested was the Manual Control code. Utilizing the test harness, the arm was initialized to zero angle settings for all three joints, as described above, using the 1D Interactive feature of MAX. The Combined Control code was started and the Manual Control code master switch was placed in the ON position. All three joints were powered up using the isolation switches and a series of simultaneous movements and velocity changes were used as the profile. Table 7 provides the series of commands provided to the robotic arm. Figure 53, Figure 54, and Figure 55, below, provide the Desired (commanded) and Actual (output) positions and velocities for the shoulder, elbow, and wrist joints, respectively. In all three cases, the joint motors responded well to the command inputs, showing no degradation even with all three joints online. Of note, the Actual Velocity matches the Desired only during a positional change and Desired Velocity is entered as an absolute and translated by the controller based on relative location to the Desired Angle.

The single disparity in this test shows up on the right side of the Angular Velocity plot for the Elbow (Figure 54, bottom right). There are two spikes in the Desired Velocity even though Elbow movement is stopped. This discrepancy comes from one of the Wrist joint air pads being improperly aligned and introducing a minute frictional force during Shoulder movement which caused the Elbow to initiate motion to hold position. Alignment of the air pads alleviated the divergence, but the inadvertent discrepancy proves that the system will adjust to maintain a commanded value.

Table 7 Manual Control Code Test Profile

Joint	Command	Notes
Shoulder	-20 degrees, 3 degrees/s	Initial set velocity at power up
	1.25 degrees/s	
	-37 degrees	
	-2 degrees, 2.5 degrees/s	Velocity change after move starts.
Elbow	5 degrees/s	Initial set velocity at power up
	4 degrees/s	
	15 degrees	
	9 degrees/s, changed to 4 degrees/s	
	-50 degrees, 9 degrees per second	Velocity change after move starts
	0 degrees, 3.5 degrees/s	
Wrist	3.75 degrees/s	Initial set velocity at power up
	2.5 degrees/s	
	-22 degrees	
	-0.5 degrees, 3 degrees/s	Velocity change after move starts

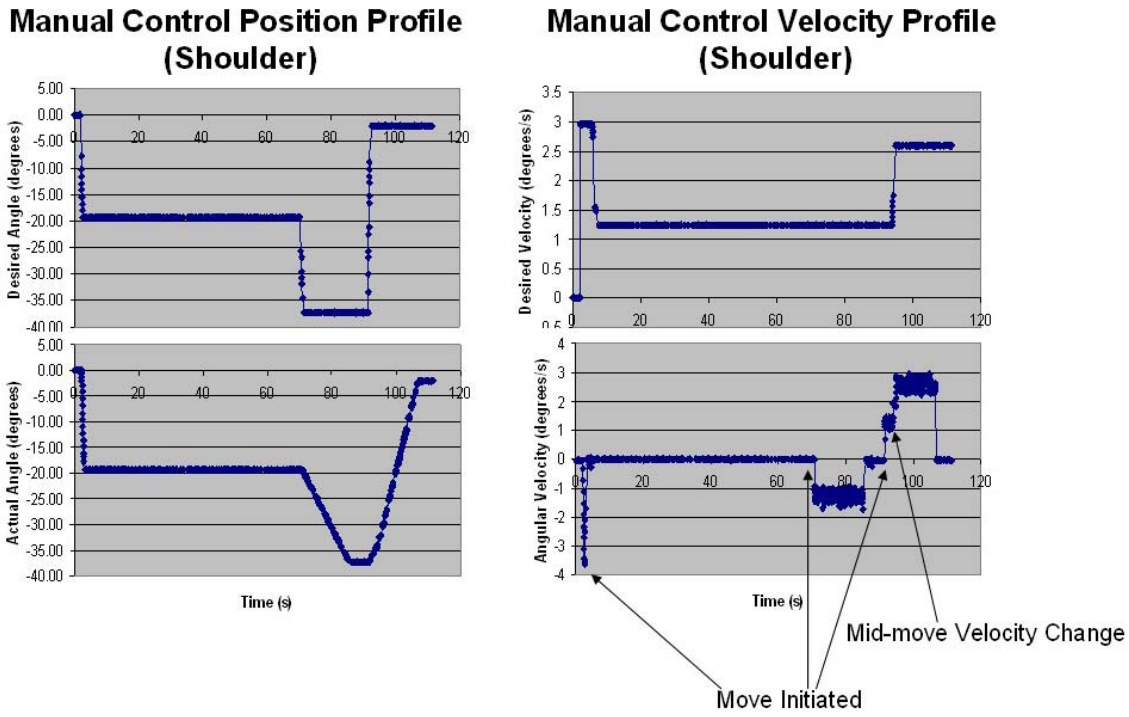

Figure 53 Manual Control Profile for Shoulder Joint

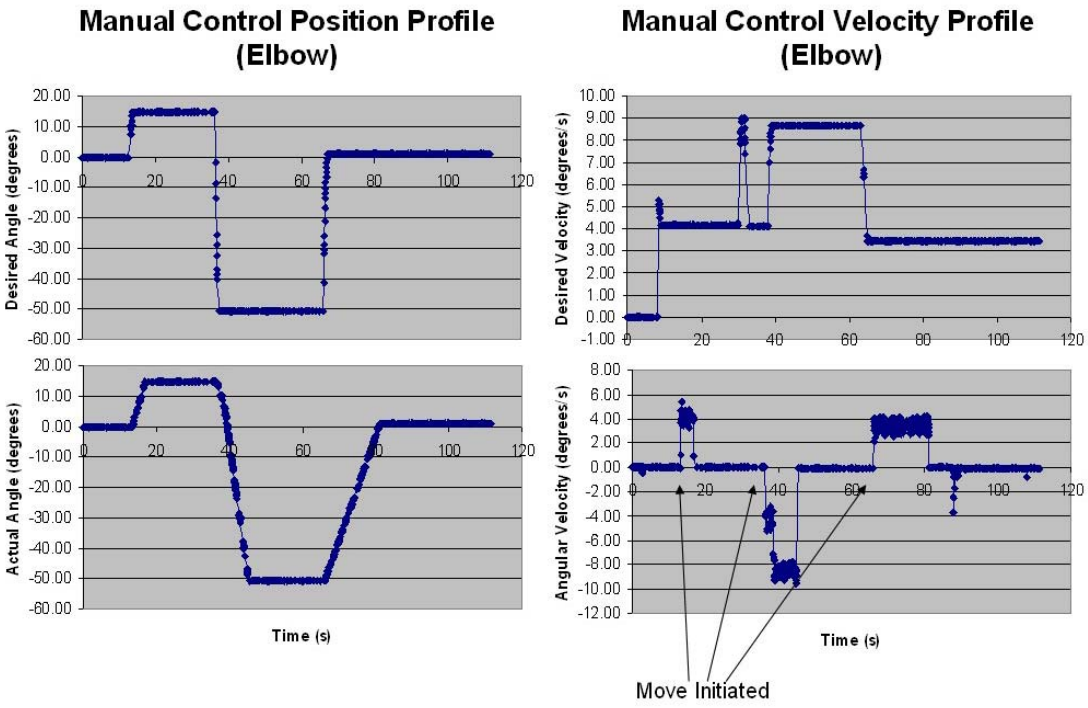

Figure 54 Manual Control Profile for Elbow Joint

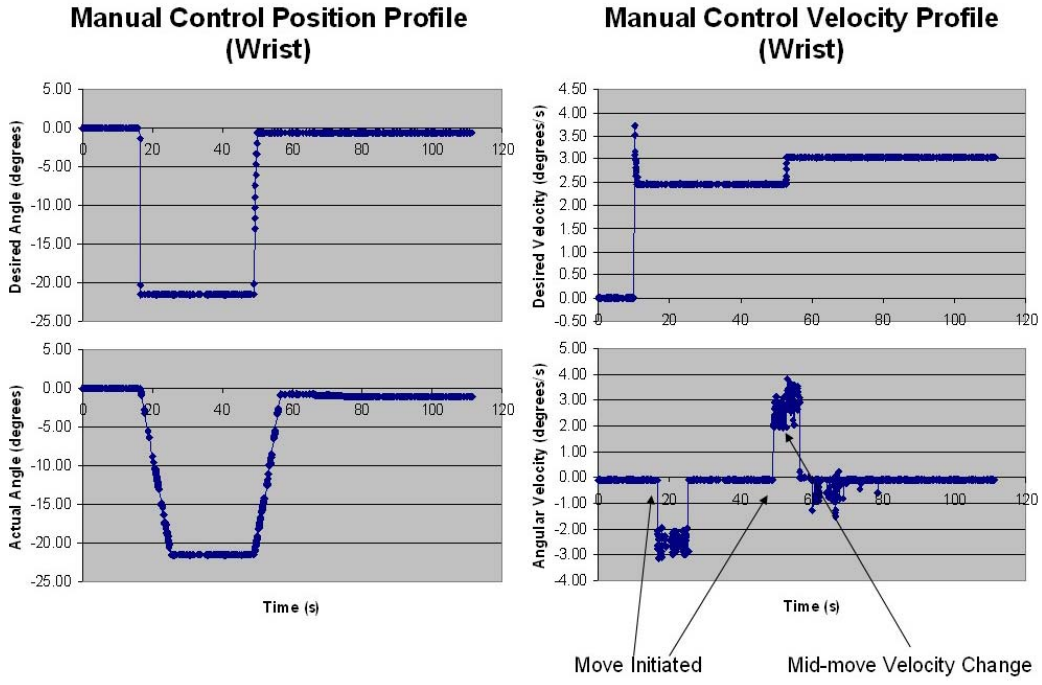

Figure 55 Manual Control Profile for Wrist Joint

2. Home Finder Performance

The single function tested on the NPADS main body was the Home Finder algorithm. MAX was used to initialize the robotic arm in a false zero reference frame to prove that the zero position would be reset during the algorithm. Testing occurred on the vehicle to verify that the stowed position of the arms would not negatively impact any of the arm or vehicle assemblies.

As described in Chapter III, the right Shoulder joint was moved in the positive direction until contact was made with the Home Switch, Shoulder position was reset to the correct zero reference position, and then the procedure was repeated for the Elbow. Figure 56 shows the position of the Home Switch (i.e., On or Off) and the movement of the two joints. As illustrated, the Shoulder is reset to 158 degrees (175,500 counts) and the Elbow to -118 degrees (-65,750 counts). Figure 57 provides the velocities of the two joints through the algorithm; as stated in Chapter III, motion occurs at fixed velocities.

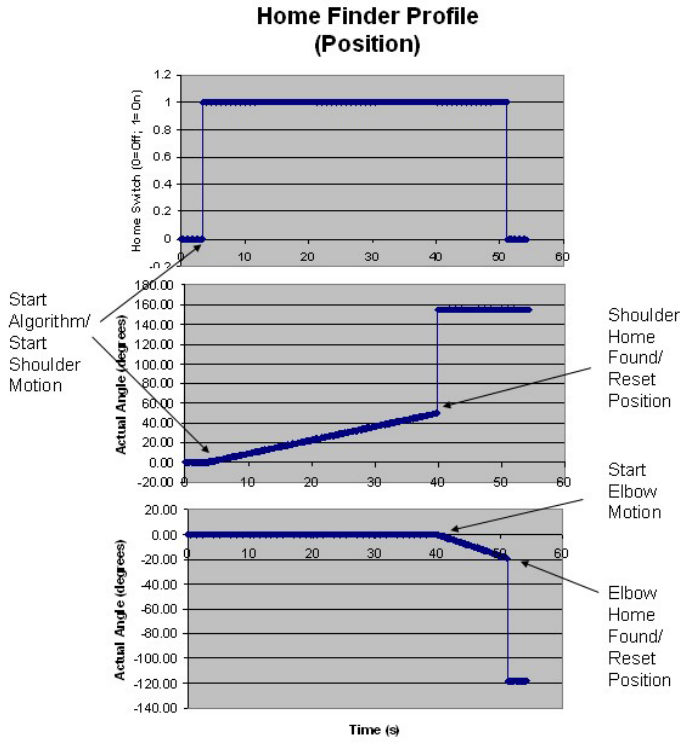

Figure 56 Home Finder Profile for Shoulder and Elbow Position

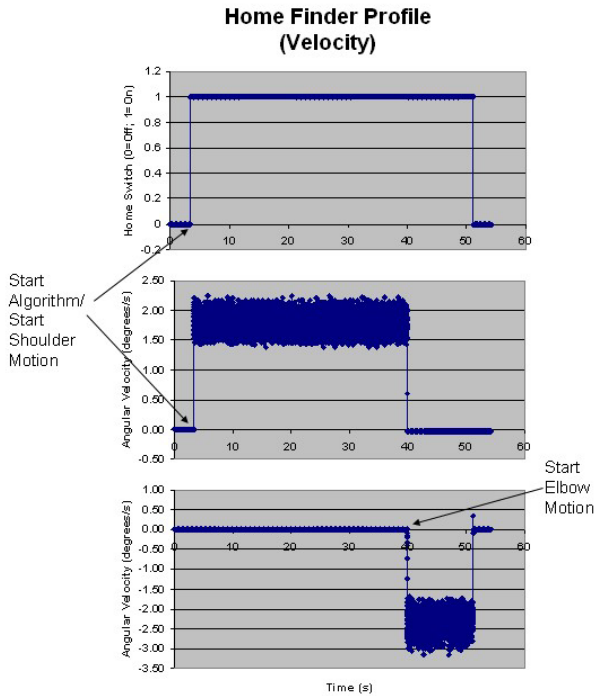

Figure 57 Home Finder Profile for Shoulder and Elbow Velocity

3. Commanded Angle Performance

Commanded Angle testing utilized the test harness. MAX was again used to set the proper zero reference condition and then the arm was moved slightly off zero. The Combined Control code was started and the Commanded Angle master switch was placed in the ON position. A series of angular commands were given to the arm using the digital controls and the GO switch. Table 8 supplies the series of commands provided to the robotic arm. Figure 58 provides the Desired Angle and the joint position and velocity response for both the Shoulder and Elbow. Both joints responded accurately.

Though not easily recognizable in the plots, the Desired Angle for the Shoulder joint actually leads motion initiation. This is due to algorithm information flow. The user enters the desired angles, obviously one at a time, then initiates motion with the GO switch. During testing, the Shoulder angle was always entered first and therefore the Desired Angle changes immediately, but the arm does not respond until the switch is toggled. And again, the velocity of each joint is held constant within the algorithm.

Table 8 Commanded Angle Control Code Test Profile

Command	Shoulder Angle (degrees)	Elbow Angle (degrees)
1	0	0
2	-30	25
3	15	-35
4	0	0

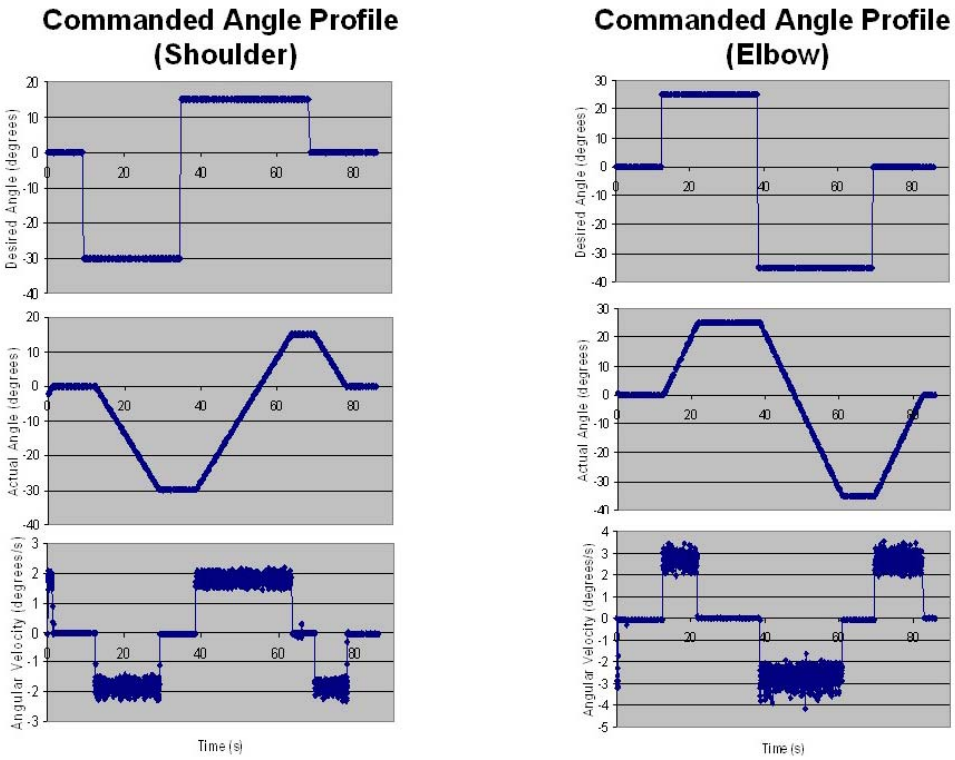

Figure 58 Commanded Angle Profile for Shoulder and Elbow

4. Commanded X-Y Performance

Commanded X-Y testing also utilized the test harness. And again, the zero reference position was initiated using MAX and the arm was moved slightly off zero. The Combined Control code was started and the Commanded X-Y master switch was placed in the ON position. Various planar positioning commands were given to the arm using the digital controls and the GO XY switch. Table 9 provides the series of positions supplied to the robotic arm. Figure 59 illustrates the path of the wrist joint as it is driven

to the Desired position. Figure 60 shows the joint position and velocity response for both the Shoulder and Elbow required to place the wrist in the Desired position.

Due to the set deadband (+/- 10 counts) of the joint motors, the actual positions vary slightly from those commanded. The deadband is a region on the encoder, defined by a motion controller default setting using MAX, within which a commanded movement is considered complete. The positional error due to this setting is within one tenth of an inch, therefore the arm joint responses are deemed adequate and accurate.

Command 6 (see Table 9) was included to test system response to an illegal command, one beyond the reach of the arm. As shown, even though the command was given, the arm remained motionless as anticipated. The Desired X position suffers from the lead time issue discussed in the previous section, since all positions were entered X, then Y prior to GO XY initiation. Once again, the absolute velocity of each joint is held constant within the algorithm.

Table 9 Commanded X-Y Control Code Test Profile

Command	Wrist X Position (inches)	Wrist Y Position (inches)
1	0	20.5
2	-20	4
3	-2	15
4	-10	12
5	2	18
6	21	18
7	0	20.5

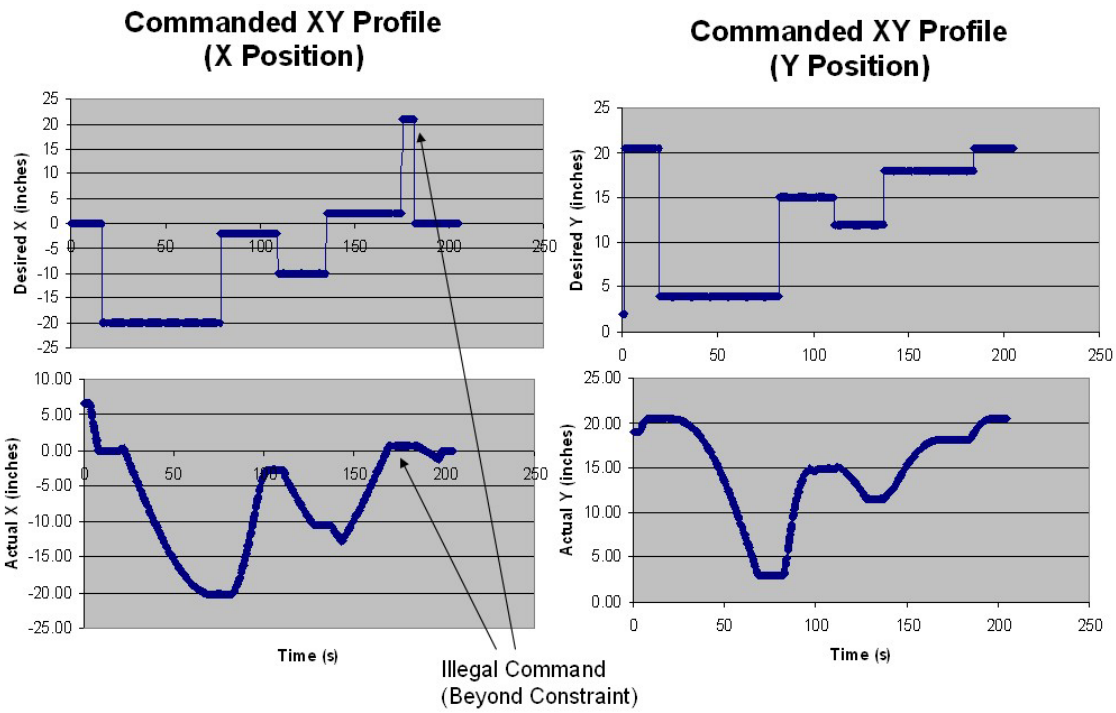

Figure 59 Commanded X-Y Profile for Wrist Position

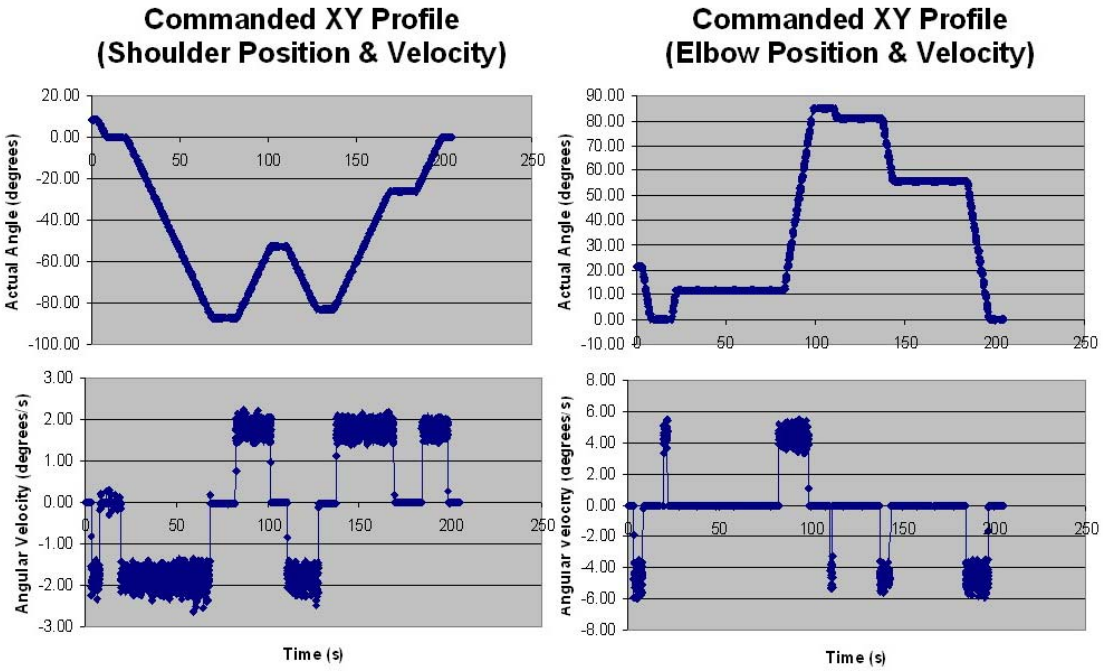

Figure 60 Commanded X-Y Profile for Shoulder and Elbow

5. Visual Target Acquisition Performance

The vision-based Target Acquisition algorithm was tested primarily to establish a reliable conversion factor, as discussed in Chapter III, which allowed for an accurate distance measurement of a circular target from the camera boresight (or center of the wrist joint) within the range of motion allowable from the fixed base test harness. A solid black circle, six and a quarter inches in diameter, was used as a primitive target. Measurements were taken at two extreme positions, straight out (all joints at the zero position, 46-1/4 inches boresight to target) and fully extended left (Shoulder at -90 degrees, Elbow at 0 degrees, and Wrist at 90 degrees, 66-1/2 inches boresight to target), using a variety of pixels to inches conversion factors.

The initial settings at each of the two positions were based off the geometric relationship between distance from camera to target and the pixel width of the frame; however, due to curvature of the lens, a "fish-eye" effect is experienced and the snapshot has a residual curvature that produces an error in this approach. Therefore the analysis provided in Table 10 and Table 11 established the conversion factors necessary at each position (10.00 straight forward and 7.00 fully extended left). The addition of a range sensor, or possibly just a second camera, would allow a linear interpolation estimation to be made for this factor that would provide reasonably accurate X-positions on a repeatable basis.

Table 10 Visual Target Acquisition Code Test Profile (Straight Out)

Conversion Factor (pixels/inches)	Target X Distance (inches)	Visual X Distance (inches)
8.20	0	0.00
	8	9.88
	16	19.02
	-8	-9.51
	-24	-26.20
8.60	0	0.00
	8	9.19
	16	18.26
	-8	-9.30
	-24	-25.58
10.00	0	0.00
	8	8.30
	16	15.80
	-8	-8.10
	-24	-27.50

Table 11 Visual Target Acquisition Code Test Profile (Fully Extended Left)

Conversion Factor (pixels/inches)	Target X Distance (inches)	Visual X Distance (inches)
5.82	0	0.00
	8	9.97
	16	19.42
	-8	-9.45
	-24	-27.32
10.00	0	0.00
	8	5.70
	16	11.30
	-8	-5.50
	-24	-15.90
7.00	0	0.00
	8	8.29
	16	16.14
	-8	-8.00
	-24	-22.71

V. SUMMARY AND CONCLUSIONS

A. SUMMARY

The objective of this thesis was to develop a set of robotic arms for the NPS Planar Autonomous Docking Simulator (NPADS) servicing vehicle by designing a motion control system, manufacturing a skeletal support structure, integrating the mechanical and electronic components, and constructing the control software necessary to operate the system. Off-the-shelf hardware components were used to facilitate development, since the purpose of the simulator is to provide a test bed for further research. Following wiring and integration of the various third party components, the National Instruments LabVIEW suite was used to develop the various algorithms for control of the robotic arms. Manual control was developed first to test system integrity; then, a series of autonomous control subroutines were created to provide functionality within the overall control program of the NPADS vehicle. Incorporation of a wrist mounted camera enabled the arms to provide a limited, stand alone input for autonomous operation. This research provided two robotic arms ready for integration onto the servicing vehicle, integration of grappling mechanisms or manipulators, or testing of advanced control algorithms.

B. FOLLOW-ON RESEARCH

1. Improvements

The following improvements to the NPADS robotic arms, servicing vehicle, and test facility are recommended:

- Define the method of command for the robotic arms, and integrate the autonomous control algorithms into the servicing vehicle control code. Currently, one arm is mated to the servicing vehicle, the other is mounted on the test harness to facilitate further testing.
- Modify the control code for the arms to act in a coordinated manner. The algorithms built for this thesis are capable of being modified to allow this type

of operation. Coordinated control would assist the main body control algorithm by counteracting the torque effects of a single arm in motion as well as providing the basis for coordinated grapple and capture approaches.

- Develop a vision algorithm for the servicing vehicle targeting camera such that it can provide target position information as well. Once the wrist camera and servicing vehicle targeting camera are working in concert, develop an algorithm to localize position of the target in two dimensions. Implementation of some form of range finder may be necessary.

- Develop a larger air-bearing surface on which to conduct operation of the simulator. With the addition of the robotic arms, the granite table will soon become restrictive. To act as a proper test bed for testing rendezvous and capture devices, the NPADS system will need a significantly larger area in which to operate.

- Develop a capture method using the robotic arms to initiate docking with a target vehicle. Though the NPADS vehicle can act as a test bed for advanced capture devices, a simple method must be devised in order to test docking devices alone.

2. Future Work

The addition of robotic arms to the NPADS vehicle greatly increases the capability of the simulator and moves one step closer to providing an operational test bed. As stated above, now that the arms are functional, it is critical to integrate the NPADS system into a single set of control laws. Once the controls are unified, perhaps a more efficient means of autonomous control can be developed using advanced programming techniques, such as fuzzy logic or neural networks, so that the simulator can adapt as it operates. Further, the robotic arms open a plethora of research opportunities at NPS (and elsewhere) in development of dexterous manipulators, capture devices, docking mechanisms, and smart targets.

The vision of the simulator was to provide a system that would prove the necessity of a revolution in satellite design. Building satellites that could have much

longer life expectancy due to repair and refueling by a system such as this is an important consideration from both operational and engineering standpoints. This fact opens up other areas of continued research, including space operations and architecture, operations analysis, systems engineering, and risk assessment. The NPADS system provides the potential for many future research opportunities that will support a variety of Department of Defense issues and interests among numerous academic disciplines.

THIS PAGE INTENTIONALLY LEFT BLANK

APPENDIX A: STRUCTURAL DRAWINGS

As mentioned in Chapter II, the joint motor support structures, or joint motor housings, were constructed using 6061-T6 Aluminum. The Figures that follow provide the mechanical specifications for the individual pieces that comprise the housings and linkages. The housings were designed such that the joint motors are securely stationed in a fixed position to ensure positional repeatability. The open architecture provides heat dissipation as well as being light-weight.

The top plate, shown in Figure 61, is split and clamped using two 10-32 screws in order to accommodate the shape of the servo motor and increase stability. The bottom plate (Figure 62) includes mounting holes for two air pads on the elbow and wrist and a center hole that takes advantage of the hollow shaft design of the motors by allowing the air supply line for the air pads to extend through the hollow shaft and this plate. Figure 63 shows the standoffs for the two housing types (shoulder and elbow/wrist). The shoulder housing has shorter standoffs since there is no need to use the hollow shaft for air supply. The elbow and wrist housings also include a back plate, shown in Figure 64, which firmly attaches to the joint motor housing with seven 10-32 screws and the linkage to the previous joint, with four additional 10-32 screws. Figure 65 shows the arm linkages, with eight mounting holes, for M6 screws, to the output shaft of the joint motor and a larger hole central to these eight which allows access to the joint motor hollow shaft. At the opposite end of the linkage are the four mounting holes which attach at the back plate and a cutout in the bottom of the channel that enables the joint motor power and feedback lines to lie inside the channel as well.

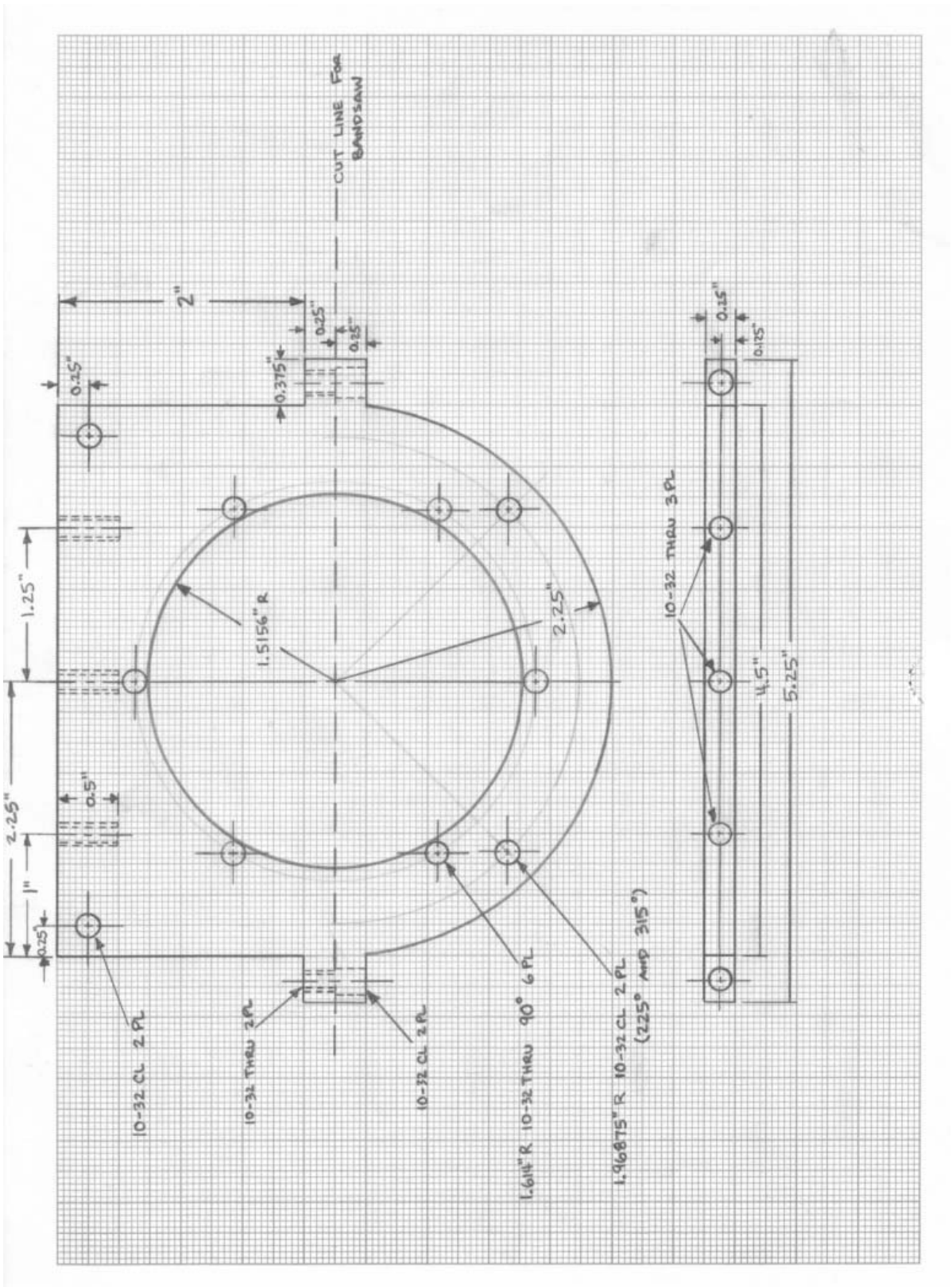

Figure 61 Joint Motor Housing Top Plate

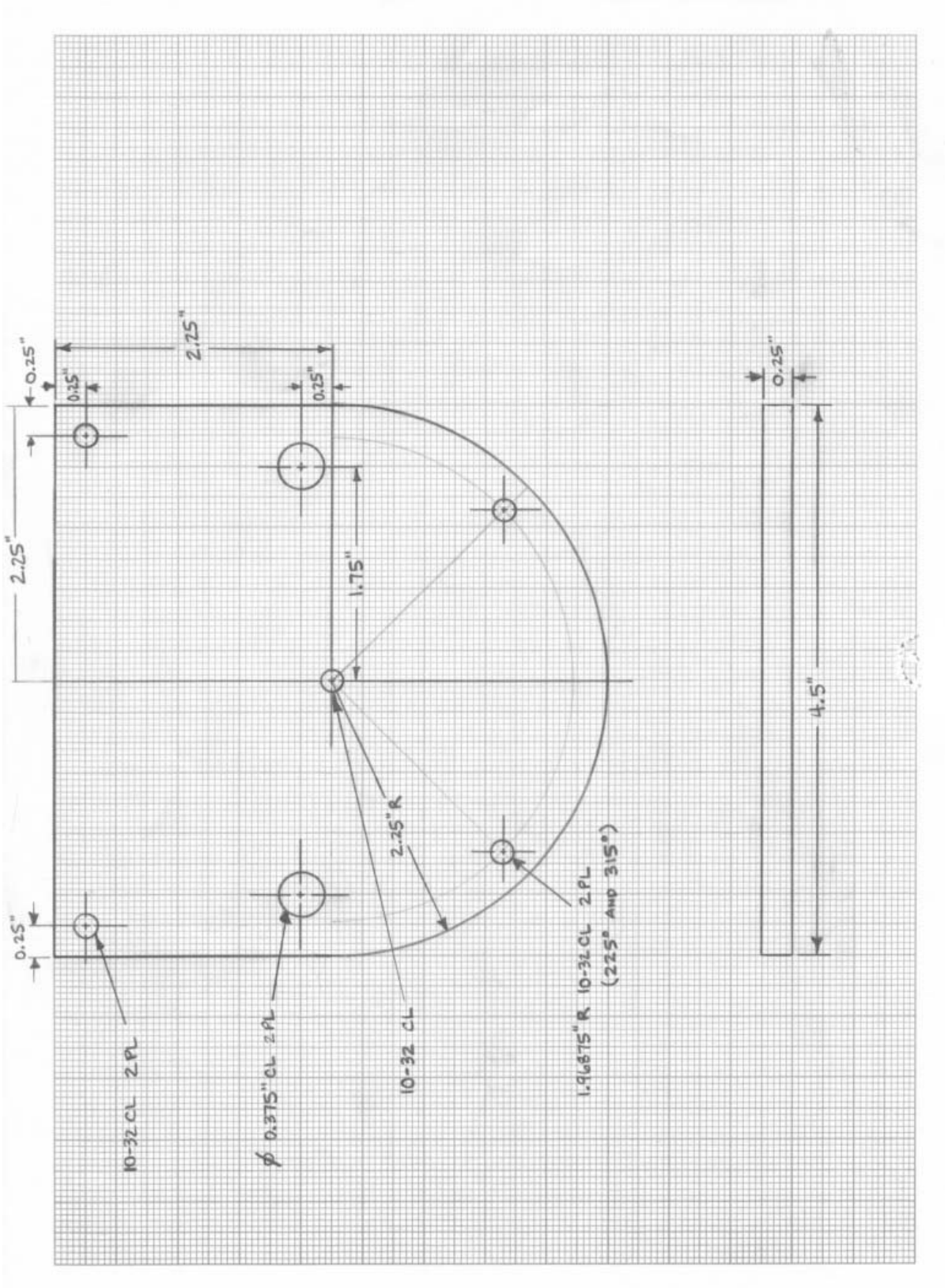

Figure 62 Joint Motor Housing Bottom Plate

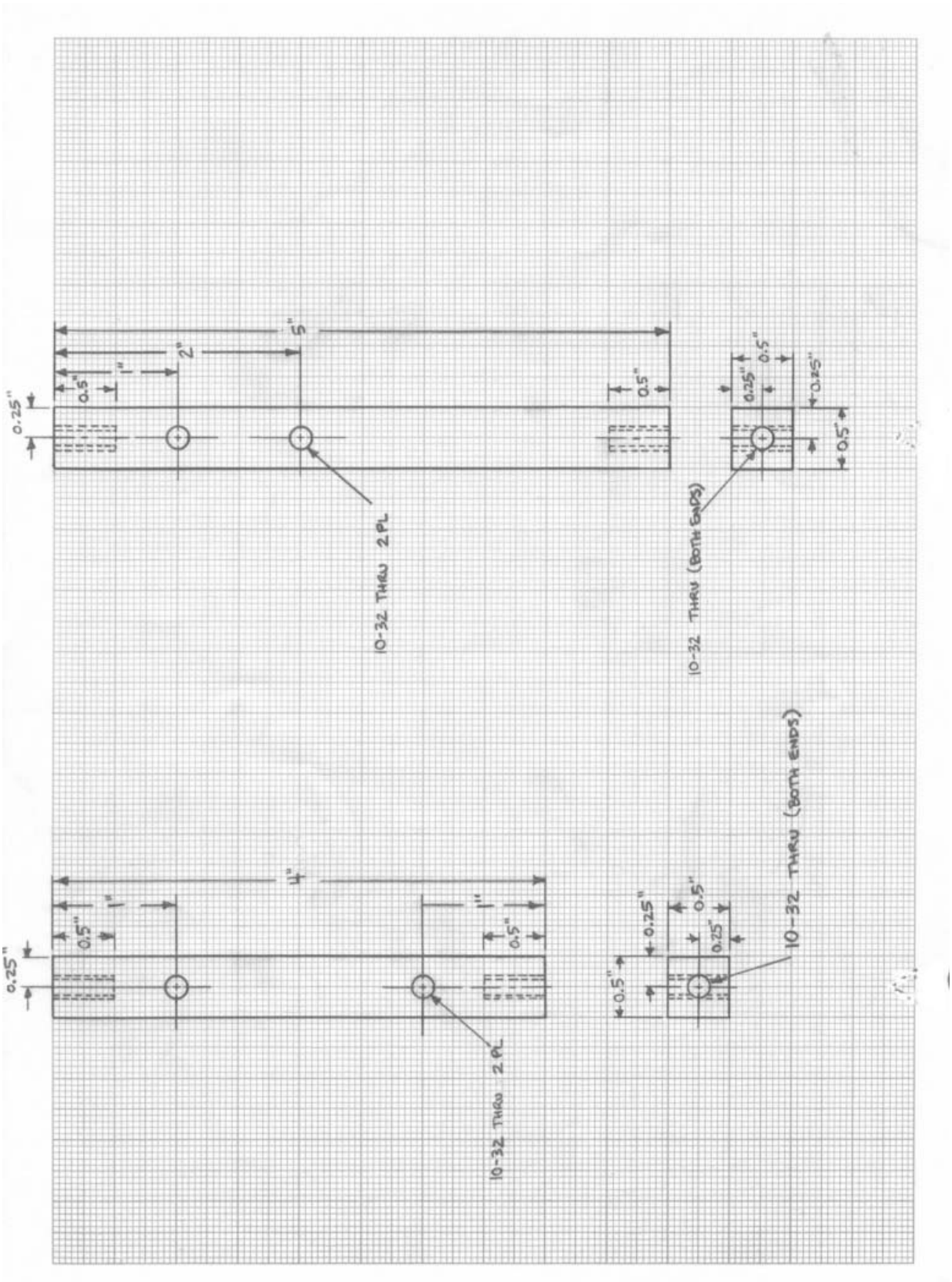

Figure 63 Joint Motor Housing Standoffs (Shoulder, short; Elbow/Wrist, long)

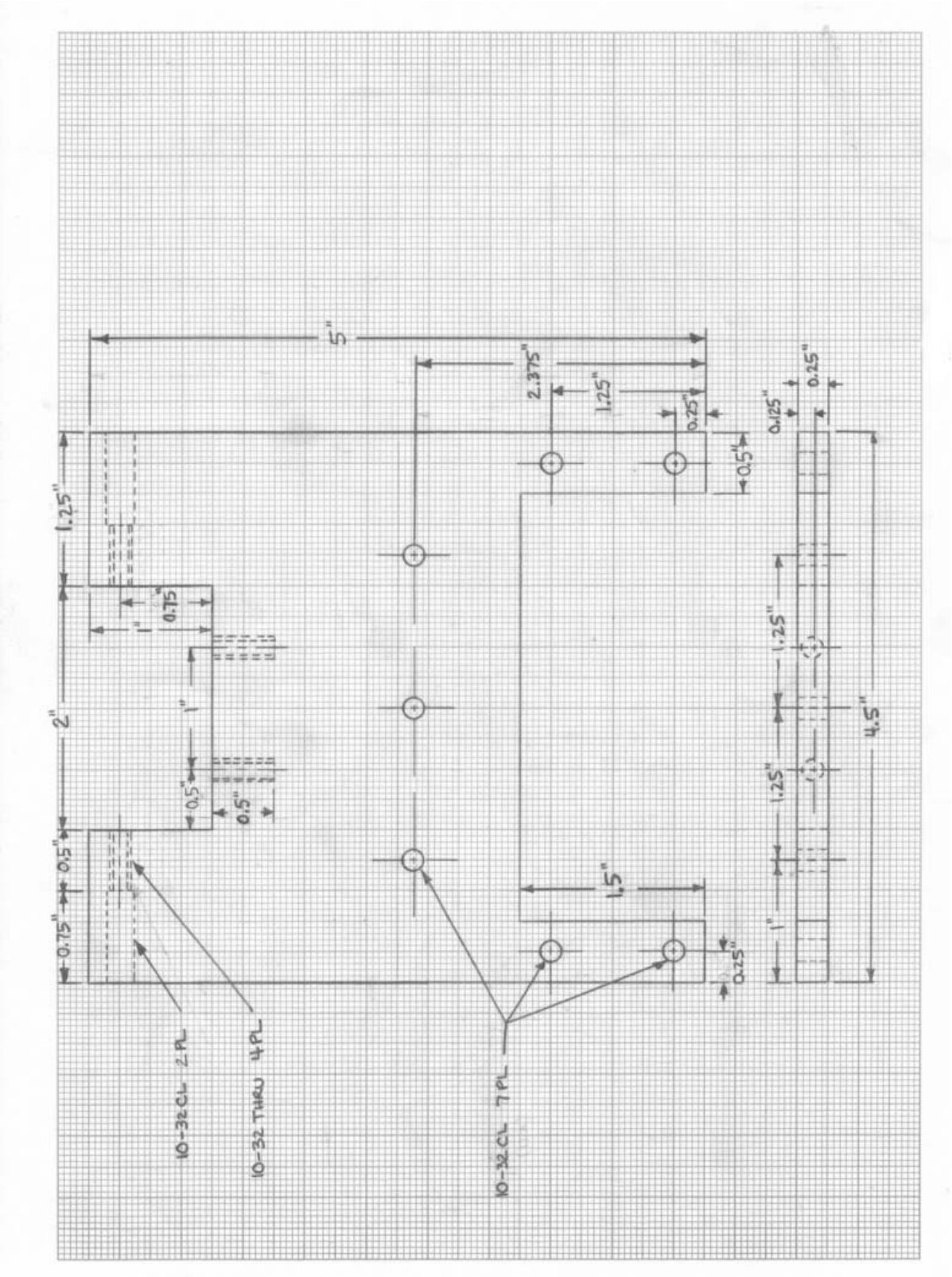

Figure 64 Elbow/Wrist Joint Motor Housing Back Plate

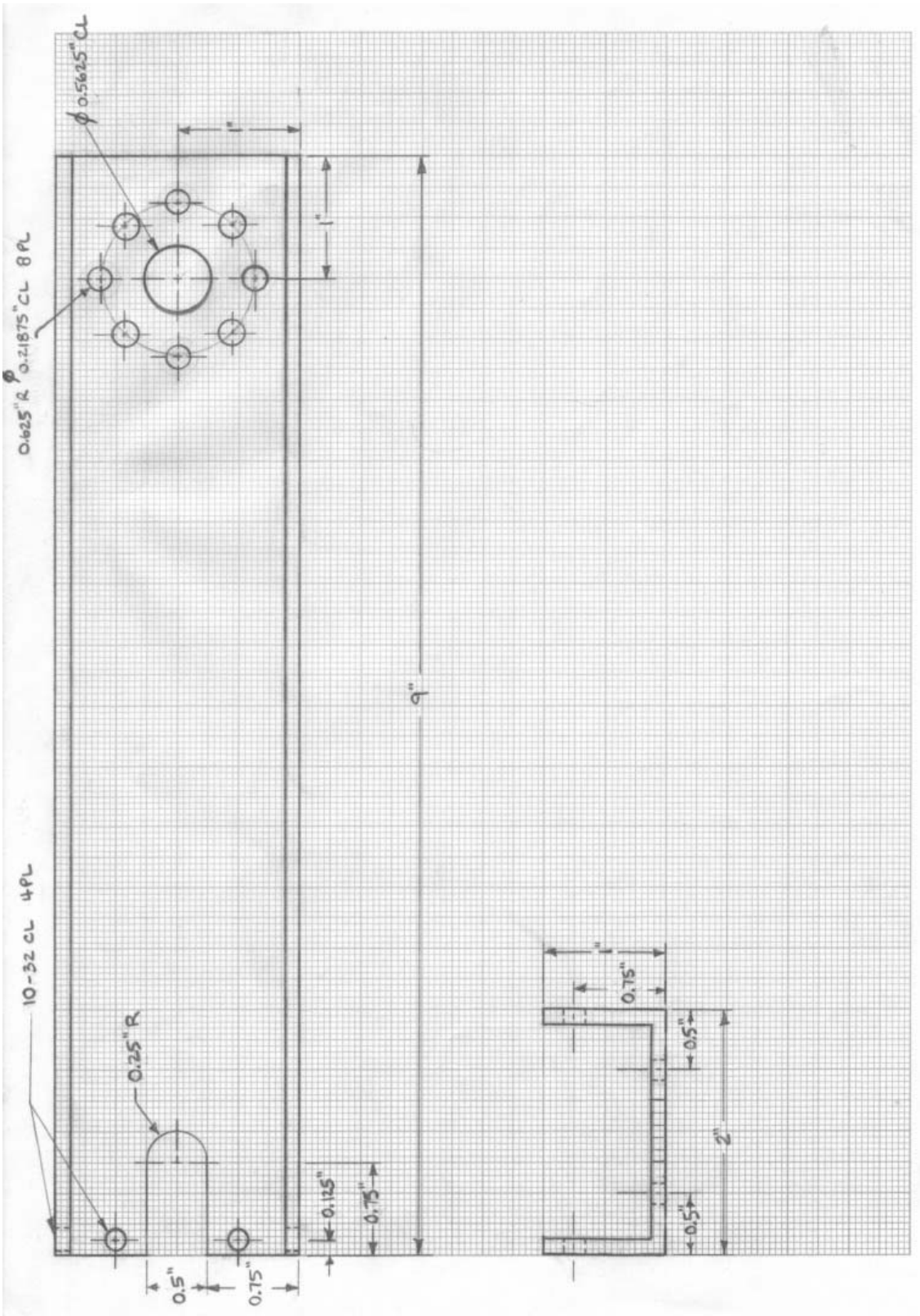

Figure 65 Arm Linkage

APPENDIX B: WIRING SPECIFICATIONS

Due to the interaction of the various pieces of the motion control system, a common wiring scheme was developed. Beginning with the two integrated wiring harnesses (power and feedback) coming from the joint motors, the following figures and tables provide the electrical path for each of the signals necessary to control the robotic arms. Figure 66 illustrates the pin location (looking toward the pins on the male connector, opposite numbering for the female receptacle) for the standard AMP connectors used on the joint motors. The motor power cable uses AMP 206705-2 and the feedback cable uses AMP 206152-1. Table 12 provides the pinout for the two cables (Note: wire colors are not included, the first three motors were checked and a different color scheme was used for each – the pins are standard though).

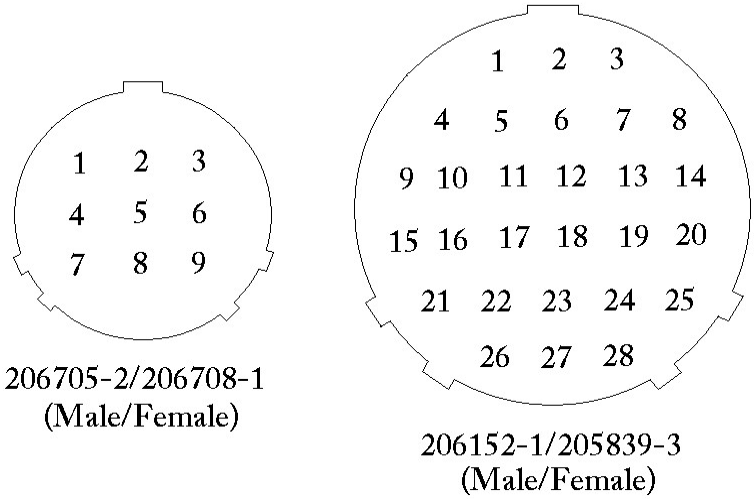

Figure 66 AMP Connector Pinouts

Table 12 Motor Connector Pinout

POWER		FEEDBACK	
Function	**Pin #**	**Function**	**Pin #**
Phase A	1	Hall Sensor 1	15
Phase B	2	Hall Sensor 2	19
Phase C	3	Hall Sensor 3	17
Shield/GND	5	GND	23
[redacted]		5V	22
		Encoder A	9
		Encoder A-	10
		Encoder B	12
		Encoder B-	11
		Encoder I	13
		Encoder I-	14
		Shield	24

The electrical path for motor power (24 V) travels from the batteries, through the isolation switches discussed in Chapter II, to the amplifier, and, finally, to the joint motor. Table 13 provides the pinout of the harness connecting the servo amplifier and joint motor power cable.

Table 13 Motor Power Cable to Amplifier Harness Pinout

Function	**Wire Color**	**Socket #**	**Connects To**
Phase A	White	1	Motor A (amplifier)
Phase B	Green	2	Motor C (amplifier)
Phase C	Red	3	Motor B (amplifier)
Shield/GND	Black/Shield	5	Grounding Screw (amplifier)

Further, in order to facilitate modularity and connection between components, a series of harnesses were developed to break out the feedback lines needed by the UMI and the amplifiers. Figure 67 shows the pin location of the MOLEX connectors used to split the feedback path (again, looking toward the pins on the male connector, opposite numbering for the female receptacle). Table 14 provides the wiring arrangement for the

intermediate harnesses connecting motor feedback cables with UMIs and amplifiers. Figure 68 shows another standard MOLEX connector used to connect the feedback line to the amplifier. Table 15 illustrates how this connector is used and provides the pinout for the servo amplifiers.

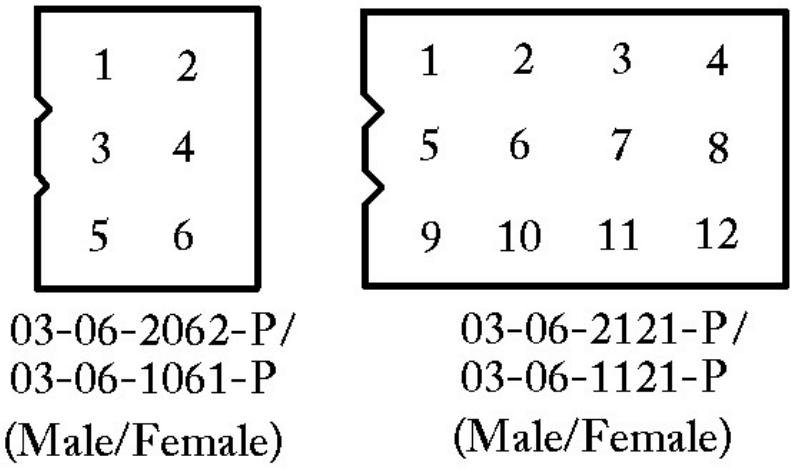

Figure 67 MOLEX Connectors Pinouts for Feedback Harnesses

Table 14 Motor Feedback to UMI/Amplifier Harness Pinout

Function	Wire Color	Socket #	To Amplifier Pin #	To UMI Pin #
Hall Sensor 1	Green	15	5	
Hall Sensor 2	Green-White	19	3	
Hall Sensor 3	Green-Black	17	1	
GND	Orange (White-Black)[1]	23	2	8
5V	White	22		4
Encoder A	Red	9		1
Encoder A-	Red-White	10		5
Encoder B	Red-Black	12		9
Encoder B-	Blue	11		2
Encoder I	Blue-White	13		6
Encoder I-	Blue-Black	14		10
Shield	Shield/White-Black	24		11
Analog GND	Black[2]		4	7
Analog Output	Orange-Black[2]		6	3

1 White-Black Connects Amplifier Ground with UMI Ground (Common)
2 Analog Signal from UMI (Controller) to Amplifier

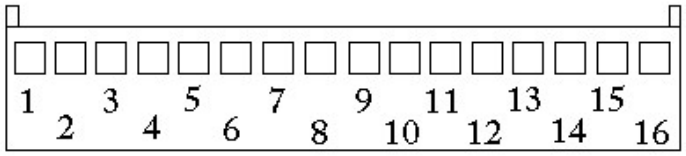

Figure 68 MOLEX Connector for Amplifier Pinout

Table 15 B12A6L Servo Amplifier Pinout

Connector	Pin	Function	Wire Color/Notes
P1 (Figure 68)	1	+10V@3mA OUT	NOT USED
	2	SIGNAL GND	White-Black (Ties to UMI GND)
	3	-10V@3mA OUT	NOT USED
	4	+REF IN	Orange-Black (Analog OUT from UMI)
	5	-REF IN	Black or Black-White (Analog GND from UMI)
	6	-TACH IN	NOT USED
	7	+TACH/GND	NOT USED
	8	Current Monitor OUT	NOT USED
	9	INHIBIT IN	NOT USED
	10	+V HALL OUT	NOT USED
	11	GND	NOT USED
	12	HALL 1 IN	Green
	13	HALL 2 IN	Green-White
	14	HALL 3 IN	Green-Black
	15	Current REF OUT	NOT USED
	16	FAULT OUT	NOT USED
P2 (Screw Terminals)	1	MOTOR A	White (Phase A)
	2	MOTOR B	Red (Phase C)
	3	MOTOR C	Green (Phase B)
	4	POWER GND	Grey (Terminal 6 or 11, Table 2)
	5	HIGH VOLTAGE	Yellow (Terminal 5 or 10, Table 2)

Figure 69 shows the internal layout of the Universal Motion Interface. The UMI requires a 5V input so that it can provide a 5V output through Terminal Screw #5 (this provides power to the joint motor Hall Sensors, which in turn provide commutation feedback to the amplifiers). Table 16 provides the UMI wiring pinout required for each joint motor. The UMI communicates these signals to the 7344 Motion Control Board using a 68-pin I/O cable (National Instruments Part #SH68-C68-S).

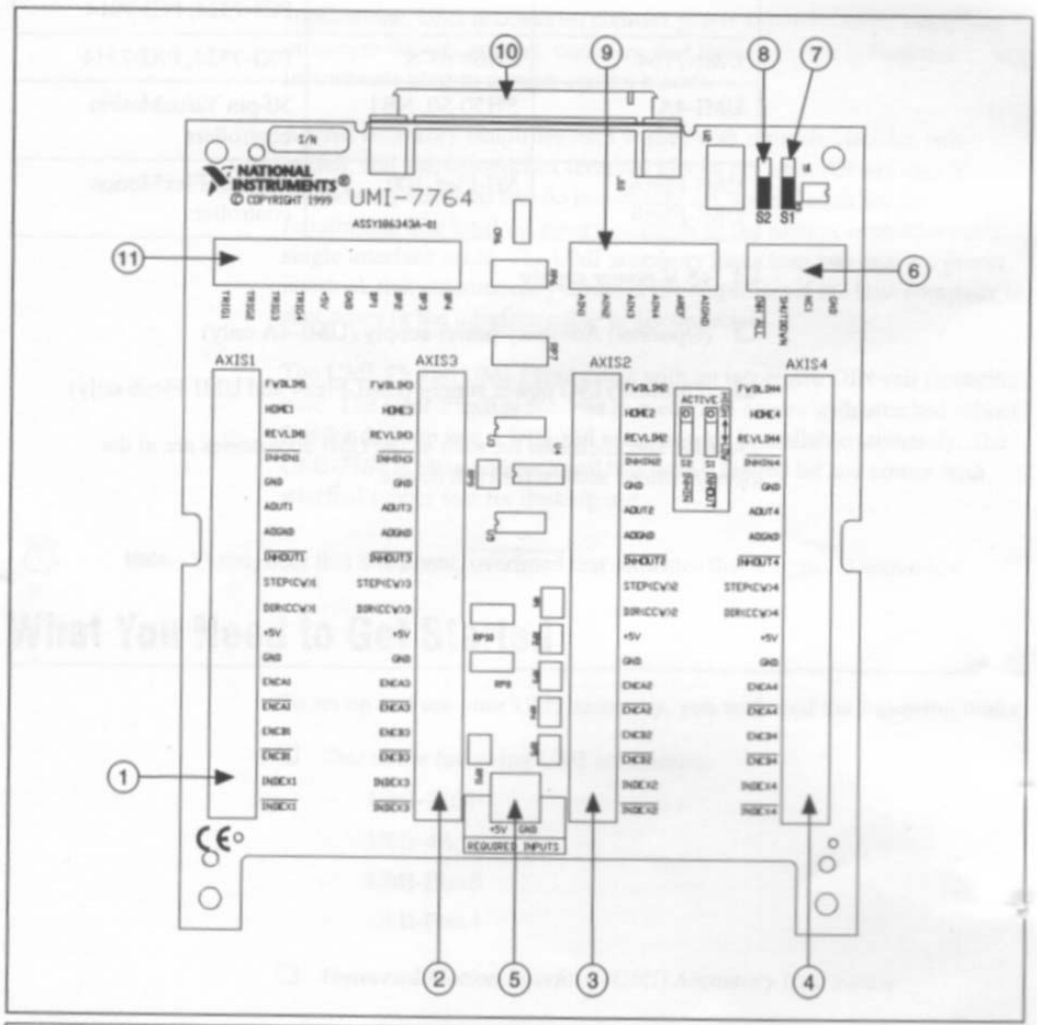

1	Axis 1 Motion I/O Terminal Block	5	Power Input Terminal Block	9	Analog Input Terminal Block
2	Axis 3 Motion I/O Terminal Block	6	Shutdown/Inhibit All Terminal Block	10	68-Pin Motion I/O Connector
3	Axis 2 Motion I/O Terminal Block	7	Inhibit Output Polarity Switch (S1)	11	Breakpoint/Trigger Terminal Block
4	Axis 4 Motion I/O Terminal Block	8	Inhibit Input Polarity Switch (S2)		

Figure 69 UMI Layout (From: Ref. 6)

Table 16 UMI Pinout Per Axis

Terminal Screw #	Function	Wire Color
1	Forward Limit	NOT USED
2	Home Input	White[1]
3	Reverse Limit	NOT USED
4	Inhibit Input	NOT USED
5	Digital GND	White-Black/SHD and Black[1]
6	Analog OUT	Orange-Black
7	Analog Output GND	Black
8	Inhibit Output	NOT USED
9	Step (CW)	NOT USED
10	Dir (CCW)	NOT USED
11	+5V OUT	White
12	Digital GND	Orange
13	Encoder Phase A	Red
14	Encoder Phase A-	Red-White
15	Encoder Phase B	Blue
16	Encoder Phase B-	Red-Black
17	Encoder Index	Blue-White
18	Encoder Index-	Blue-Black

1 Home Switch Harness – only on shoulder (Axis 1) and elbow (Axis 4)

APPENDIX C: MOTION CONTROLLER SETTINGS

A. DEFAULT 7344 SETTINGS

Table 17, on the following pages, provides a page by page listing of required settings for 7344 Motion Controller initialization, using the Default 7344 Settings option of the Measurement & Automation Explorer (MAX). These settings are utilized by either arm. Not all settings are listed for every page. For those not listed, default values are used. Formatting for the table as compared to the MAX interface is shown in Figure 70.

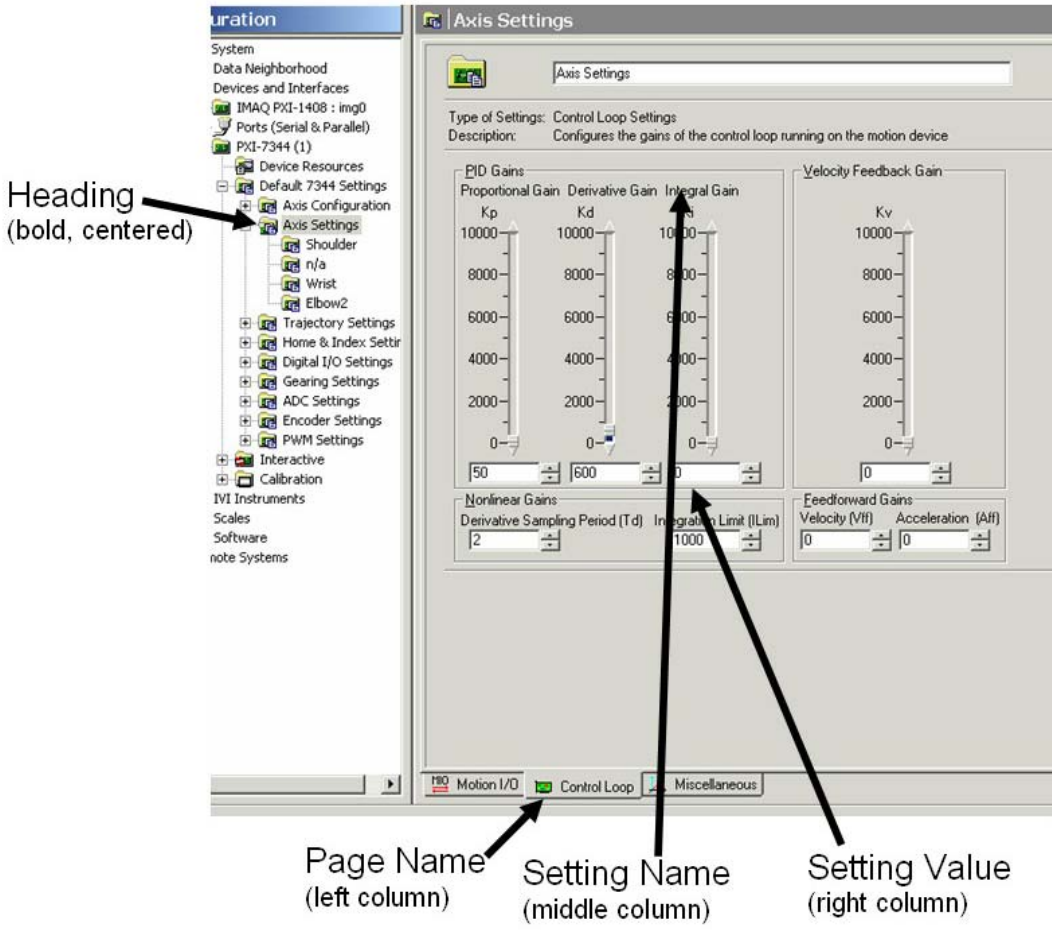

Figure 70 MAX Default 7344 Settings Definitions

Table 17 Default 7344 Settings

Axis Configuration		
Axis Configuration	*Axis Type*	Servo
	Axis Enabled [1]	Enabled (1,3, and 4) Disabled (2)
	Encoder & Stepper Resolution *(Encoder counts per revolution)*	Axis 1: 400,000 Axis 3,4: 200,000
	Axis Resources & Update Period *(Control Loop Update Period)*	188 microseconds
	Axis Resources & Update Period *(Primary Feedback)*	Encoder 1, 3, and 4, respectively
	Axis Resources & Update Period *(Primary Output)*	DAC Channel 1, 3, and 4, respectively
	Axis Resources & Update Period *(Secondary Feedback)*	None
	Axis Resources & Update Period *(Secondary Output)*	None
Axis Settings		
Motion I/O	*Home & Limit Switch Settings* *(Forward Limit Switch)*	Disabled
	Home & Limit Switch Settings *(Reverse Limit Switch)*	Disabled
	Home & Limit Switch Settings *(Home Switch)*	Enabled, Active Low Polarity
	Software Limit Settings *(Forward Software Limit)*	Axis 1: Disabled Axis 3: Enabled, 60,000 counts Axis 4: Enabled, 66,000 counts
	Software Limit Settings *(Reverse Software Limit)*	Axis 1: Disabled Axis 3: Enabled, -60,000 counts Axis 4: Enabled, -66,000 counts
	Inhibit Output Settings	Disabled
Control Loop	*ALL VALUES*	See Table 18 for values from Calibration/Servo Tune
Miscellaneous	*Load Torque Limits & Offsets in:*	Volts
	Primary DAC Output *(Positive Torque Limit)*	10 Volts
	Primary DAC Output *(Negative Torque Limit)*	-10 Volts

	Primary DAC Output *(Torque Offset)*	0 Volts
Trajectory Settings		
Trajectory Settings	*Operation Mode*	Velocity
	Stop Mode	Kill
	Load Velocity in:	counts/s
	Velocity	2500 counts/s
	Advanced Move Settings *(Velocity Threshold)*	38,000 counts/s
Move Complete Criteria	*Deadband*	10 counts
Home & Index Settings		
Home & Index Settings	*Reset Position After:*	Never
Digital I/O Settings		
Digital I/O Settings	*ALL*	Defaults
Gearing Settings		
Gearing Settings	*Gearing Enabled*	Disabled
ADC Settings		
ADC Settings	*Channel*	1,3,4: Enabled 2: Disabled
	ADC Range	-10 to +10 Volts
Encoder Settings		
Encoder Settings	*Encoder*	1,3,4: Enabled 2, Disabled
	Filter Frequency	1,3,4: 400 KHz
PWM Settings		
PWM Settings	*PWM*	Disabled

1 Enables only active axes: Axis 1 (shoulder), Axis 3 (wrist), and Axis 4 (elbow)

B. SERVO TUNE GAINS

As described in Chapter III, MAX was utilized to manually tune the six brushless servo joint motors, the required gains were identified for each. Table 18 lists these gains identified for stable operation of the joint motors. Once established in Servo Tune, these values automatically save to the Default 7344 Settings/Axis Settings/Control Loop page, allowing proper initialization at power-up.

Table 18 PID Control Gains for NPADS Robotic Arms

Left Arm	Kp	Kd	Ki	Td	Right Arm	Kp	Kd	Ki	Td
Shoulder	25	275	0	2	Shoulder	50	600	0	2
Elbow	85	355	0	2	Elbow	15	160	0	2
Wrist	85	330	0	2	Wrist	50	250	0	2

As mentioned in Chapter III, MAX also contains routines to produce Step Responses, Bode Plots, and Trajectory Responses. Figure 71, Figure 72, and Figure 73 provide examples of each of these tools, respectively, for one of the joint motors. Due to the low speed, high torque operation expected of the joint motors, Step Response was the primary driver of the tuning process. Adjusting the gains allowed for minimization of the Maximum Overshoot and Settling Time, ensuring optimum performance and limited vibration of the motors.

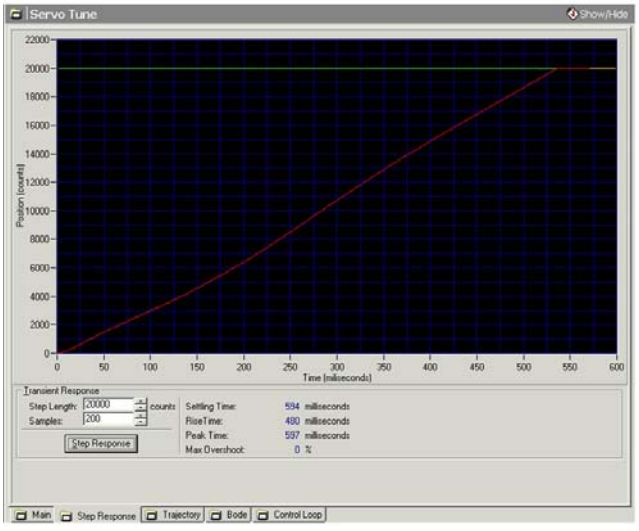

Figure 71 MAX Step Response Plot

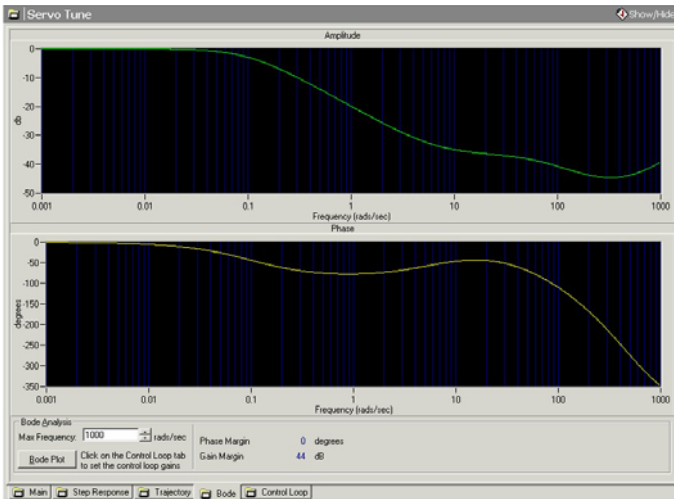

Figure 72 MAX Bode Plot

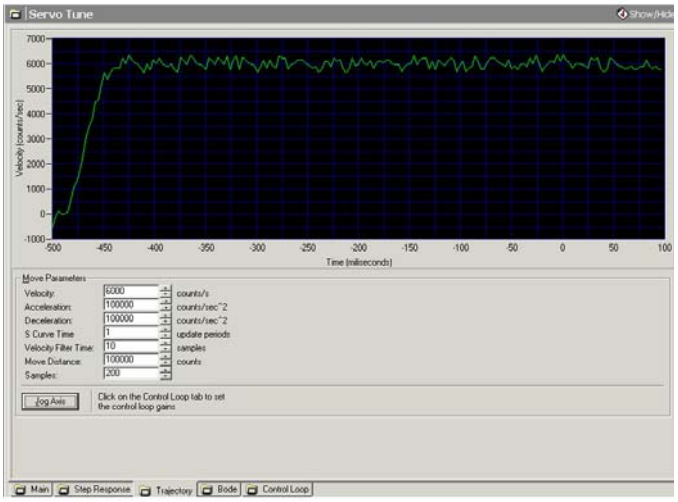

Figure 73 MAX Trajectory Response Plot

THIS PAGE INTENTIONALLY LEFT BLANK

LIST OF REFERENCES

1. Yoshida, Kazuya, "Space Robot Dynamics and Control: To Orbit, From Orbit, and Future," presented at the International Symposium on Robotics Research, 9th, Snowbird, Utah, October 1999.

2. "The Special Purpose Dexterous Manipulator (SPDM)," [http://www.space.gc.ca/csa_sectors/human_presence/iss/contribut/mss/spdm/default.asp], 17 September 2001.

3. "Robonaut," [http://vesuvius.jsc.nasa.gov/er_er/html/robonaut/robonaut.html], 05 February 2001.

4. Porter, Robert D., *Development and Control of the Naval Postgraduate School Planar Autonomous Docking Simulator (NPADS),* Master's Thesis, Naval Postgraduate School, Monterey, California, September 2002.

5. Harmonic Drive Technologies Motor Specifications, *PowerHub™ Harmonic Drive Servo Actuator,* February 2000.

6. National Instruments, *Universal Motion Interface (UMI) Accessory,* August 1999.

7. National Instruments, *Motion Control: 7344/7334 Hardware User Manual,* August 2001.

8. National Instruments, *IMAQ: IMAQ PCI/PXI™-1408 User Manual,* October 1999.

9. National Instruments, *PXI™: PXI-8150B Series User Manual,* February 1999.

10. National Instruments, "Understanding Servo Tune," [http://zone.ni.com/devzone/conceptd.nsf/webmain/4B7775373E4AE64986256B6000691505?opendocument], 2002.

11. Chen, Chi-Tsong, *Analog and Digital Control System Design: Transfer Function, State-Space, and Algebraic Methods,* pp. 69-102, Harcourt Brace Jovanovich College Publishers, 1993.

THIS PAGE INTENTIONALLY LEFT BLANK

INITIAL DISTRIBUTION LIST

1. Defense Technical Information Center
   Ft. Belvoir, Virginia

2. Dudley Knox Library
   Naval Postgraduate School
   Monterey, California

3. Department Chairman
   Department of Aeronautics and Astronautics
   Monterey, California

4. Department of Aeronautics and Astronautics
   Professor Michael G. Spencer
   Naval Postgraduate School
   Monterey, California

5. Department of Aeronautics and Astronautics
   Professor Brij N. Agrawal
   Naval Postgraduate School
   Monterey, California

6. Department of Aeronautics and Astronautics
   SRDC Research Library
   Naval Postgraduate School
   Monterey, California

7. LT Gary L. Cave, USN
   West Palm Beach, Florida